UNIL | Université de Lausanne
Faculté de biologie
et de médecine

Centre hospitalier
universitaire vaudois

Mémoire de Maîtrise en médecine N° 189

# Identification et caractérisation de gènes suppresseurs de tumeurs dans le glioblastome

**Etudiant**
Raphaël Burger

**Tuteur**
Prof. Dr. Monika Hegi
Laboratoire de Biologie et Génétique des Tumeurs
Service de neurochirurgie
Département des neurosciences cliniques

**Expert**
PD Dr. Phillip Shaw
Institut universitaire de pathologie de Lausanne

Lausanne, Décembre 2011

# Résumé

Le glioblastome (gliome de stade IV d'après l'OMS) est la tumeur cérébrale la plus fréquente et la plus maligne. Le prognostic reste pauvre à ce jour. En effet, la survie moyenne est évaluée à 15 mois, malgré une prise en charge multidisciplinaire comportant chirurgie, chimiothérapie et radiothérapie. Différentes études ont montré une diminution de l'expression de *Wnt inhibitory factor 1* (*WIF1*) suite à différents mécanismes de régulation au niveau génétique et épigénétique. Une récente étude s'est alors concentré sur le chromosome 12 et a identifié le rôle potentiel de *WIF1* en tant que de suppresseur de tumeur. Une diminution de croissance et l'adoption d'un phénotype de sénescence a pu être observé chez des cellules tumorales transfectées exprimant *WIF1* de manière ectopique. Dans ce projet, nous avons investigué l'impact de la ré-expression de *WIF1* dans des cellules de glioblastomes afin d'observer si l'inhibition de Wnt peut conduire à la sénescence. Dans un deuxième temps, nous avons mesuré l'expression de *p21* et *c-Myc. p21* jour un rôle clé dans le déclenchement de la sénescence et est directement inhibé par *c-Myc*, lui-même cible de la voie de signalisation Wnt. Nous avons donc examiné si l'action de *WIF1* peut faire varier l'expression de ces deux gènes. Finalement, nous avons analysé l'expression de différents gènes jouant un rôle dans le mécanisme d'autophagie. En effet, il a été reporté que l'autophagie cellulaire jouait un rôle dans l'apparition de la sénescence. Nous avons alors investigué ce processus pour mettre en évidence une éventuelle association avec le phénotype de sénescence observé dans les lignées cellulaire transfectées et ré-exprimant *WIF1*.

Les clones cellulaires ré-exprimant *WIF1* ont été sélectionnés après transfection de cellules stables de glioblastome. Les analyses ont été réalisées à l'aide de qPCR (quantitative polymerase chain reaction), FACS (fluorescence-activated cell sorting) et histochimie. *IGFBP7* et *ALDH1A3* ont été choisis pour refléter la sénescence. *ATG5*, *ATG7* et *ULK3* ont été choisis pour refléter l'activité autophagique.

Nous avons observé au sein des lignées ré-exprimant *WIF1* un plus grand pourcentage de cellules agrandies, multinuclées, comportant une granularité cellulaire augmentées et positives à la beta-galactosidase, ce qui correspond aux différentes caractéristiques de la sénescence. Une augmentation de l'expression de gènes associés à la sénescence a aussi été mise en évidence dans ces mêmes lignées. Toutes ces caractéristiques ont pu être corrélées aux différents taux d'expression de *WIF1*. Nous n'avons pas remarqué d'association entre les expressions de *WIF1* et de *p21*, ni entre celles de *WIF1* et de *c-Myc*. Une correlation entre l'expression des gènes associés au mécanisme d'autophagie et de ceux associés à la sénescence a pu être observée dans une des deux lignées cellulaire analysées.

Suite à nos investigations à différents niveaux, nous avons l'évidence de l'apparition d'un phénotype de sénescence auprès des lignées cellulaire ré-exprimant *WIF1.* Ce fait permet de reconnaître un certain rôle de la voie de signalisation Wnt dans la tumorigénicité du glioblastome. Des analyses supplémentaires sont nécessaires pour investiguer par quel biais l'inhibition de Wnt conduit à l'apparition de la sénescence. Le rôle de l'autophagie dans ces cellules sénescentes reste peu clair. On peut observer des correlations au niveau transcriptionnel, laissant en effet penser à une implication de l'autophagie, cependant il est encore trop tôt pour clairement identifier la nature de ces associations. Des expériences supplémentaires sont là aussi nécessaires pour confirmer ces résultats préliminaires puis analyser la variation d'activité autophagique sur une durée de temps définie.

# Abstract

**Introduction**: Glioblastoma (WHO Grade IV glioma) is the most frequent and most malignant primary tumor of the brain. With a mean survival of 15 months despite multidisciplinary management combining surgery, chemo- and radiotherapy, the prognosis is poor. Different studies measured a down-regulation of *Wnt Inhibitory Factor 1* (*WIF1*) expression in a majority of gliobastoma due to genetic and epigenetic regulation. Recently, a focus on chromosome 12 identified *WIF1* as a potential tumor suppressor gene. In previous results, transfected glioblastoma cells with ectopic expression of WIF1 had a decreased growth rate and adopted a senescence-like phenotype. In this report, we first investigated the effect of *WIF1* re-expression in glioblastoma cell lines to see if Wnt inhibition by *WIF1* can lead to senescence. To look further, we assessed *p21* and *c-Myc* expression. *p21* has a key role in senescence onset and is directly inhibited by *c-Myc*, itself a target of Wnt-pathway. We thus looked if a variation of expression of these genes is triggered by *WIF1* activity. Finally, as autophagy is thought to play a role in senescence onset, we analyzed the expression of different autophagy genes. We therefore looked for an association between autophagy activity and senescent phenotype in *WIF1*-overexpressing cell lines.

**Methods**: *WIF1*-overexpressing clones were selected after transfection of stable glioblastoma cell lines. Analysis were made through quantitative Polymerase Chain Reaction (qPCR), Fluorescence-activated Cell Sorting (FACS) and histochemistry. *IGFBP7* and *ALDH1A3* have been selected to reflect senescence. *ATG5*, *ATG7* and *ULK3* have been selected to reflect autophagy activity.

**Results**: Using FACS analysis, we found a higher percentage of large cells with increased granularity amongst *WIF1*-overexpressing cell lines, which are characteristics of senescence. In addition, histochemistry showed a higher percentage of multi-nucleated, beta-galactosidase positive cells in the same cell lines. An increased expression of genes associated with senescence was found as well. All characteristics were correlated with levels of *WIF1* expression. We did not find any association between *p21* and *WIF1* expression. No correlation between *WIF1* and *c-Myc* expression was noticed either. In one of the two cell lines analyzed, the expression of autophagy genes showed some correlation with expression of *WIF1* and expression of genes associated with senescence.

**Discussion**: After investigations and characterizations on multiple levels, we have evidence for a senescence phenotype upon WIF1-overexpressing cell lines. This gives a role to Wnt pathway in the tumorigenicity of glioblastoma. Further experiments are required to investigate how Wnt inhibition leads to senescence. The role of autophagy in our senescent cells is here still unclear. Some correlations can be found, letting us think that there is indeed some involvement of autophagy. However, it is yet to soon to explain this relationship. Further experiments are required again to confirm the preliminary results and analyze the variations of autophagy activity within time.

**Keywords**: glioblastoma, WIF1, senescence, autophagy, Wnt pathway

# Introduction

With an incidence of 2.6 new cases for 100'000 habitants, representing 30% of cerebral tumors, Glioblastoma (WHO Grade IV Astrocytoma) is the most frequent and most malignant primary tumor of the brain.[1] Radiation and genetic predisposition are currently the only known causes. Two distinct presentations have been identified: primary glioblastomas occur de novo and represent up to 90% of glioblastomas while secondary glioblastomas develop from a lower grade glioma and represent the remaining 10%. Both patterns exhibit defined pathology with specific characteristics. Epidermal Growth Factor Receptor (EGFR) amplification (36% of cases) and loss of heterozygosity 10q (47% of cases) are two typical modifications found in primary glioblastomas whereas in secondary glioblastomas, IDH1 and p53 mutations are the most frequent genetic alterations (85% and 65% of cases respectively).[2] These alterations can already be found in a majority of precursor low-grade astrocytomas [Fig.1].

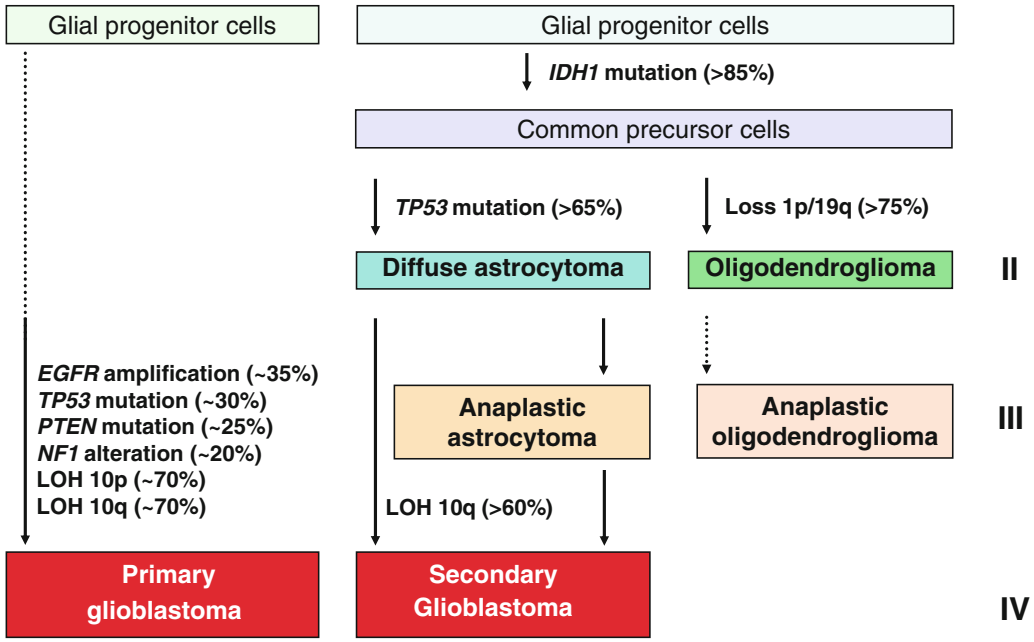


Fig. 1. Genetic pathways to astrocytic and oligodendroglial diffuse gliomas. LOH, loss of heterozygosity.[2]

Interestingly, EGFR amplification and p53 mutation are mutually exclusive, separating primary and secondary glioblastomas in two well-distinguished entities. Moreover, there is also a difference in the age distribution. The mean age for primary glioblastoma is 62

years, whereas secondary glioblastoma presents earlier, with a mean age of 45 years. These properties define two distinct pathologies, each with different evolutions, as well as different clinical profile.[3]

The current standard protocol of care is multidisciplinary, including surgical resection, radiotherapy plus concomitant and adjuvant chemotherapy with temozolomide. Despite constant improvements, the prognosis remains poor. The actual mean survival is 15 months.[4,5] There is thus a pressing need of new targets to control this deadly disease.

Lambiv *et al.* investigated the 12q13 and 12q15 chromosomal regions containing MDM2 and CDK4.[6] A gene expression-based prediction of copy number aberrations has been performed [Fig. 2] and showed a significantly lower expression of Wnt Inhibitory Factor 1 (WIF1) in glioblastoma in comparison with non-neoplastic brain tissues. This lends WIF1 a potential tumor suppressor role.

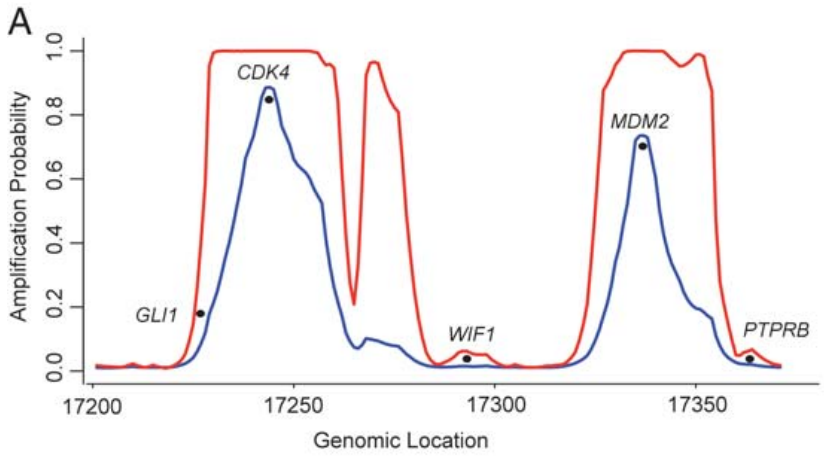


Fig. 2. Gene expression–based prediction of copy number aberrations (CNAs) in glioblastoma. (A) The maximum (red) and mean (blue) amplification probabilities on chromosome 12q14–12q15 were estimated from glioblastoma gene expression data by a hidden Markov model (HMM). The interrogated region flanked by CDK4 and MDM2 encompasses a ~11 Mb window.[6]

Wnt signaling plays an important role in embryonic development but is also known for having a strong association with oncogenesis.[7] Wnt takes part in two different pathways. The canonical one is ß-catenin dependent [Fig. 3]. When no ligand activates Frizzled, the receptor, ß-catenin is sequestered in the cytoplasm and led to proteolysis by a complex including APC, AXIN and GSK-3ß. The activation of the receptor by Wnt ligand leads to inhibition of this complex, allowing ß-catenin to translocate into the nucleus and induce transcription.

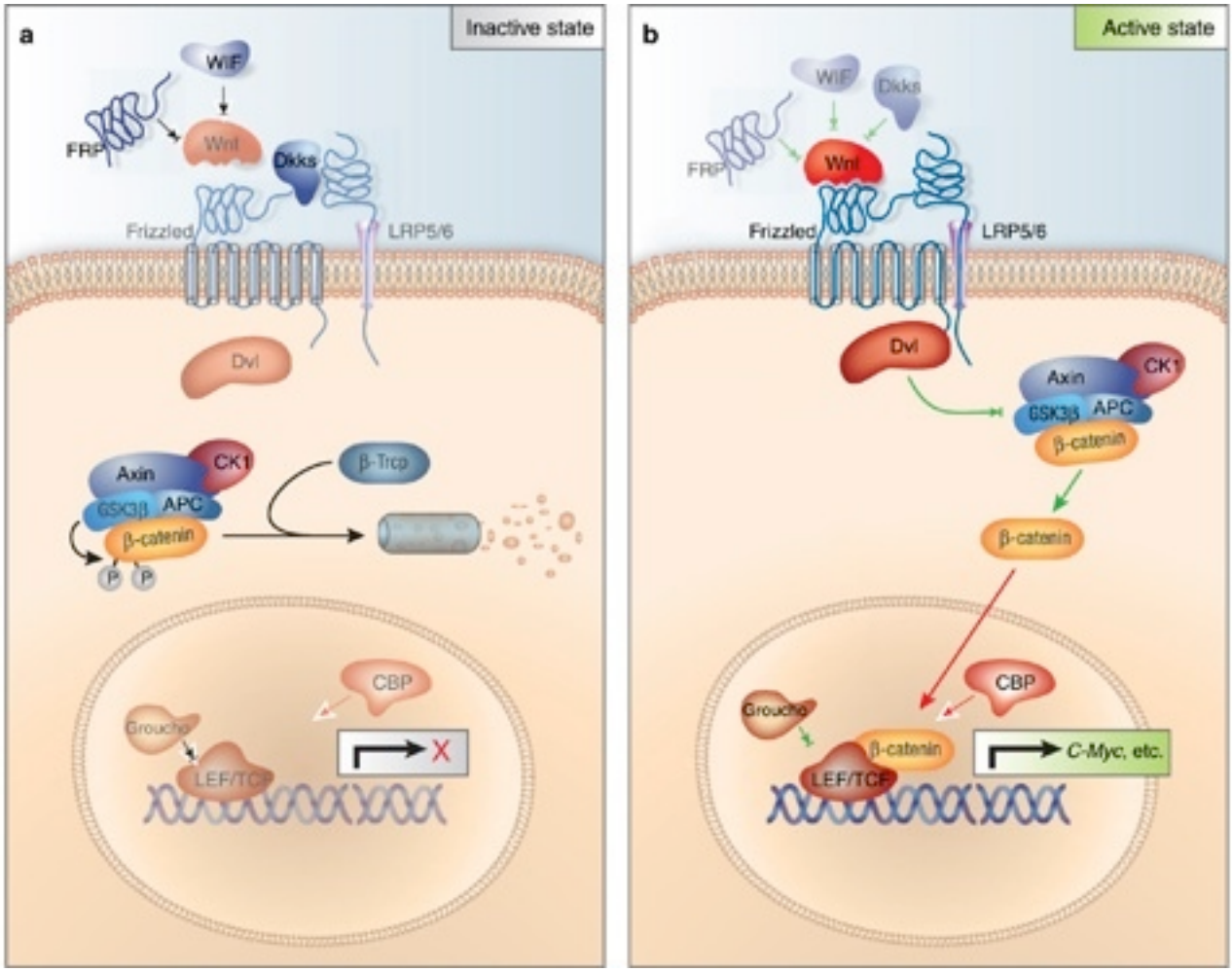


Fig. 3. (a) When no ligand binds the receptor (Fz), ß-catenin is complexed by APC, AXIN and GSK-3ß and thus sequestered and destroyed in the cytoplasm. (b) once Wnt ligands binds Fz, AXIN and GSK3ß are recruited, the complex is inhibited, allowing ß-catenin to translocate in the nucleus and induce transcription.[8]

The non-canonical pathway is ß-catenin independent and works through other components. WIF1 mechanism of action includes binding of Wnt ligand, therefore preventing its activation of the canonical Wnt signaling. Genetic and epigenetic regulation of WIF1 such as promoter hypermethylation, deletion or histone acetylation, were found in a majority of gliobastomas[9, 10, 11] and put in association with a down-regulation of WIF1 expression. This supports the candidature of WIF1 as a tumor suppressor gene. WIF1 over-expressing cells were later obtained by transfecting WIF1 into LN319 glioblastoma cells [Fig. 4]. Investigations showed a loss of Wnt pathway activity, along with a decreased growth rate. At confluence, the cells adopt a large, flat morphology[6] referring to what we know to be senescence phenotype.

In this report, we used polymerase chain reaction (PCR), histochemistry and fluorescence-activated cell sorting (FACS) to investigate the effect of WIF1 re-expression in glioblastoma cell lines. The aim was to test the ability of WIF1 to lead to senescence by inhibiting Wnt signaling.

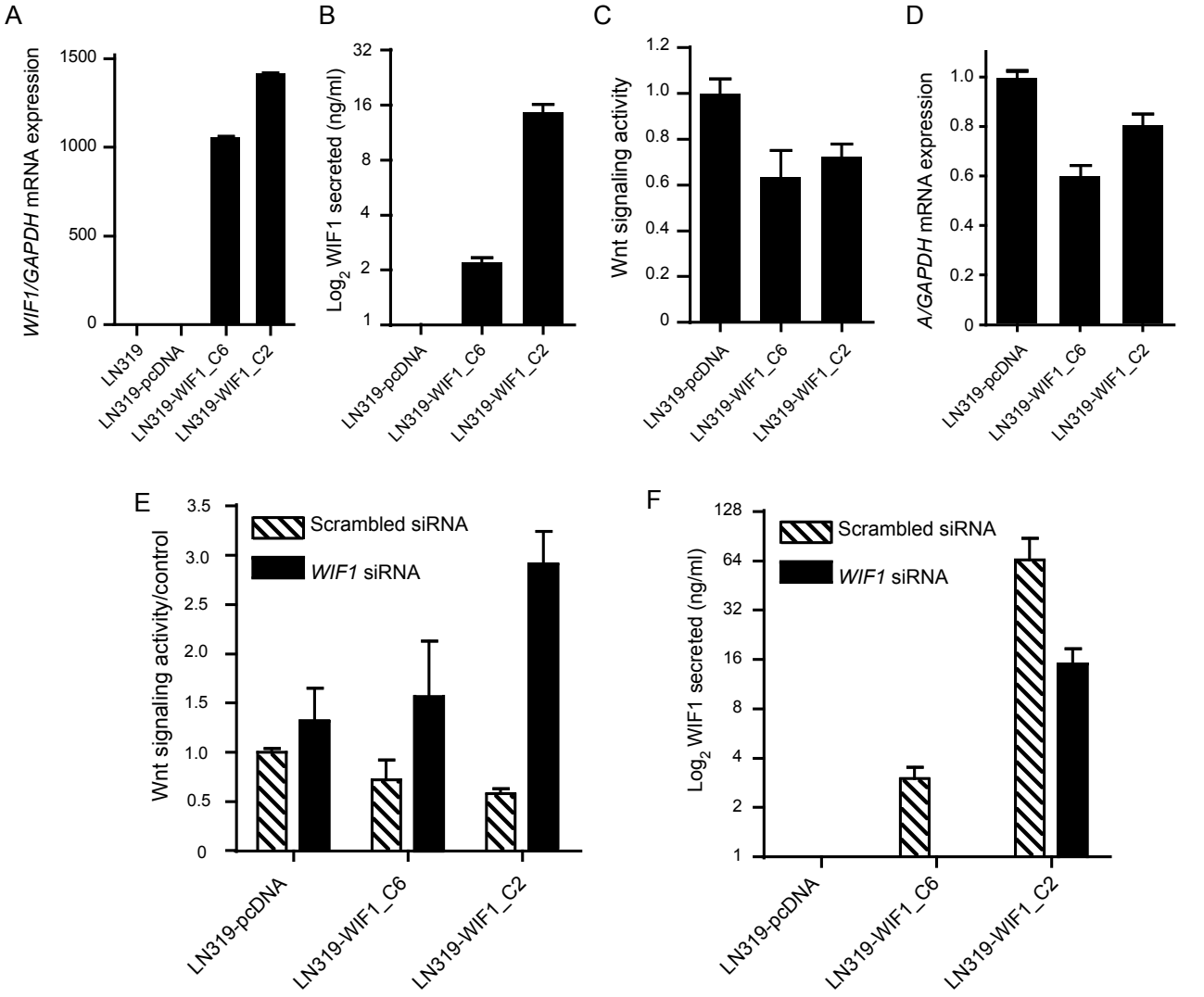


Fig. 4. LN319 cell clones stably transfected with WIF1 show reduced Wnt pathway signaling. Two stably transfected LN319 clones were analyzed for WIF1 expression by qRT-PCR (normalized to the control cells transfected with the empty vector, pcDNA3.1) (A) and WIF1 secretion by enzyme-linked immunosorbent assay (ELISA) (B). Wnt pathway signaling was measured both with the TCF luciferase reporter (TOP5/FOP5) and normalized to the control cells (C) and by measuring AXIN2 mRNA expression (D). The specificity of the WIF1-induced effects in the 2 clones was controlled by transfection of specific siRNAs against WIF1 or a respective scrambled control. Wnt pathway signaling was measured using the TCF reporter (E) and WIF1 secretion using ELISA (F). Results are marked with 1 asterisk (*) if P,.05 and 2 (**) if P,.01.[6]

In order to further understand how Wnt inhibition leads to senescence, we assessed expression of p21 and c-Myc. p21 plays a key role in the control of cell cycle as well as in the onset of senescence. It is however down-regulated by c-Myc,[12] a direct target of Wnt

signaling. The goal was to see if there is a decreased, respectively increase in c-Myc and p21 expression after inhibition of Wnt by WIF1.

Additionally, in order to investigate the onset of senescence in WIF1-overexpressing cells, we focused on another cellular process: autophagy. Autophagy is a genetically regulated mechanism characterized by the formation of double-layered cytosolic vesicles, so-called autophagosomes, and responsible for an increased turnover of cellular components. Autophagy is regulated by mTOR, which inhibits autophagy induction. In case of nutrient depletion or oncogenic stress, mTOR is inhibited, allowing early autophagy genes like ULK3 (homolog to ATG1) to start the process[13] [Fig. 5]. Although autophagy onset requires a large group of genes, ATG5 and ATG7 however were reported to be essential for autophagy to be efficient.[14] This program is thought to play a crucial role for cell survival, especially when fast metabolic changes occur. It is for example the case in early neonatal period but it can be due to any other metabolic stress. It also assures a certain quality control of cellular components and would improve the immune response to pathogens.[15]

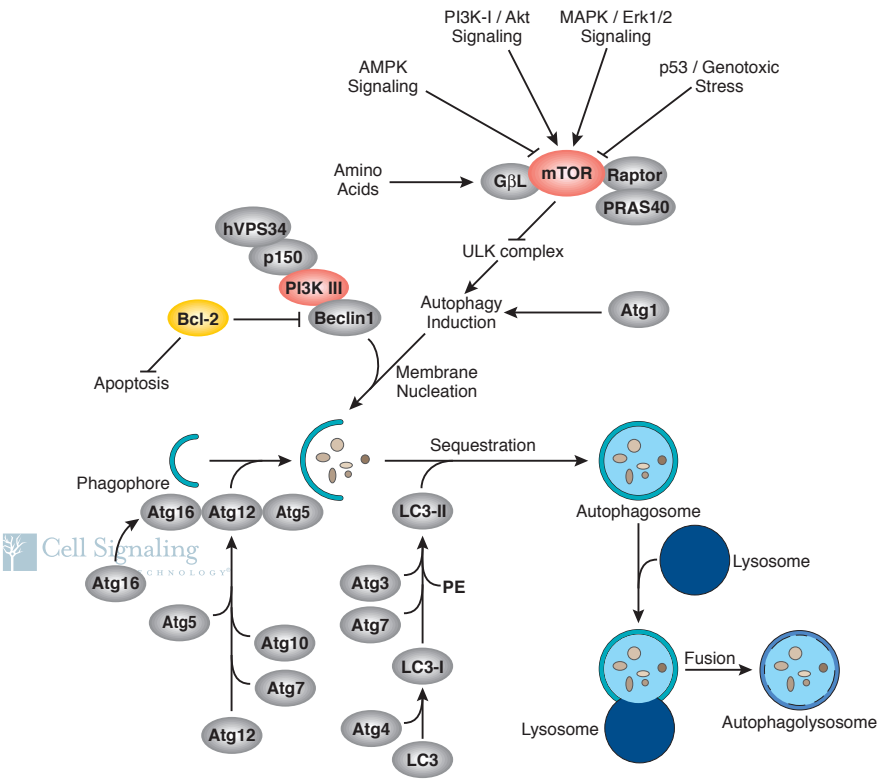


Fig. 5. When activated, mTOR inhibits autophagy. In case of nutrient depletion, genotoxic- or oncogenic stress, mTOR is inhibited, allowing early autophagy genes to start the process. ATG5 and ATG7 take place later in the cascade and are referred as essential for the effectiveness of the process.[16]

However, beside its pro-survival function, autophagy was also shown to have some association with cell death on one hand and senescence on the other.[17] The correlation between autophagy and apoptosis is not completely understood yet due to common regulating factors and common components.[15] Nevertheless, Young & Narita recently reported autophagy as a transition before entering a state of oncogene-induced senescence.[18] In human diploid fibroblasts (HDFs), an oncogenic stress triggers transiently mTor activation. Later, mTor activity decreases, allowing autophagy to become activated and the cells undergo senescence [Fig 6].

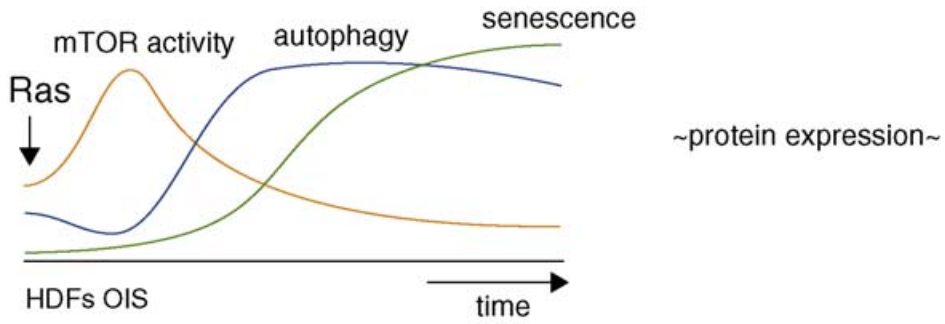


Fig. 6. Upon constitutive activation of ras, human diploid fibroblasts (HDFs) undergo oncogene-induced senescence (OIS) after the transient activation mTOR, a negative regulator of autophagy. Consistently, autophagy becomes activated upon the down-regulation of mTOR activity. During this process, cells exhibit drastic morphological changes and produce a large amount of secretory proteins. Apparently, the global rate of protein synthesis is also elevated, thus highly efficient protein turnover might facilitate the acute switch in phenotype during OIS. (Note that the time scale of each condition is not proportional.)[18]

We investigated the transition of WIF1-overexpressing cell lines into a senescence-like phenotype using ATG5, ATG7 and ULK3 expression to reflect autophagy activity. As markers for senescence, two genes were assessed: IGFBP7, part of the IGF pathway and ALDH1A3, part of the IFN pathway. Both pathways are known to regulate senescence.[19] This transition was found in non-cancerous cells but not yet in glioblastoma cells. It could be therefore relevant to understand what role WIF1 has in senescence onset.

# Methods and materials

*Glioblastoma cell lines*

Glioblastoma cell lines LN229 and LN319 were established in the Laboratory of Brain Tumor Biology and Genetics, Neurosurgery, Lausanne University Hospital. All glioma cell lines have been characterized for a defined set of molecular aberrations[20] and were con-

trolled by DNA fingerprinting as described.[21] Both cell lines were cultured in Dulbecco's modified Eagle's medium (Invitrogen), supplemented with 5% fetal calf serum (Hyclone) and 100 units/mL penicillin, 100 units/mL streptomycin (Invitrogen). WIF1 was subcloned into the vector pIRES2-EGFP and used to transfect LN229. LN319 was stably transfected with the WIF1 expression vector and its empty control pcDNA3.1, generous gifts from Professor Qian Tao, Cancer Center, Chinese University of Hong Kong.[22] LN229_C1C, LN229_C3A, LN229_C4B, LN229_C4D, LN319-WIF1_C2 and LN319-WIF_C6 were selected for their ectopic expression of WIF1. All clones were cultured in the same medium as above, supplemented with 8$\mu$m/ml of geneticin.

*LiCl treatment*

2 x $10^4$ cells were seeded onto 12-well plates and let at 37°C for 24h. Using a stock of 3M LiCl diluted in PBS, cells were then treated with a concentration of 30mM LiCl for 72h in previously described medium.

*RNA Isolation and Reverse Transcription PCR*

Total RNA was extracted using the RNeasy total RNA extraction kit (Qiagen), and cDNA was synthesized using Superscript RT II (Invitrogen). Real-time quantitative PCR was performed with Fast SybR Green Master Mix (Applied Biosystem) using the Rotor Gene 6000 Real-Time PCR system(Corbett Life Science). PCR reactions were run as duplicates. The temperature profile was as follows: 95°C (100 s) followed by 40 cycles at 95°C (3 s) to 60°C (20 s). The quality of the products was controlled by the melting curve. Transcript levels were normalized against human GAPDH.[23]
AXIN2 primers.[24] P21 primers: Forward: TGGACCTGTCACTGTCTTGT; Reverse: TCCTGTGGGCGGATTAG. c-Myc primers: Forward: GAGGCTATCTGCCCATTTG; Reverse: AGGCTGCTGGTTTTCCACTA. p27 primers: Forward: AGATGTCAAACGTGCGAGTG; Reverse: TCTCTGCAGTGCTTCTCCAA. The primers for ULK3, ATG5 and ATG7 were already described[13], just as IGFBP7 and ALDH1A3 primers.[25]

*Flow Cytometry Measurement of Cell Morphology*

Cells were grown until confluence detached using a solution of 2 mM ethylenediaminetetraacetic acid (EDTA) in PBS and resuspended in PBS. Cell size was evaluated by forward scatter (FS) and side scatter (SS) analysis using a Beckman Coulter

FC500 5-color analyzer. More than 1 × $10^4$ events were counted for all samples. Thresholds for FS and SS were arbitrarily defined.

*Histochemistry*

Cells were seeded onto glass coverslips coated with poly-L-lysine and cultured until confluence. Cells were stained for the activity of SA-b-galactosidase using the b-Galactosidase Staining Kit (Biovision), following the manufacturer's instructions, and counterstained with 4′,6-diamidino-2-phenylindole (DAPI). SA-b-galactosidase activity and nuclear morphology were visualized by bright field and fluorescence microscopy (Leica Leitz DMRB). Cells were scored in 10 randomly taken fields.

# Results

*LiCl treatment reverses WIF1 inhibition*

To test the effect of WIF1 on the Wnt-pathway, we modulated the activity of the pathway with Lithium-Chloride (LiCl). LiCl was shown to inhibit GSK-3ß, therefore to activate Wnt signaling.[26,27] After 72h treatment with 30mM LiCl, we measured AXIN2 expression. AXIN2 is known to be a direct target of the Wnt-pathway[28] and can reflect Wnt activity within the cell. We could observe an increased AXIN2 expression amongst all clones after treatment [Fig. 7]. The difference between treated cells and non-treated cells was more significant in LN319_pcDNA which doesn't express WIF1.

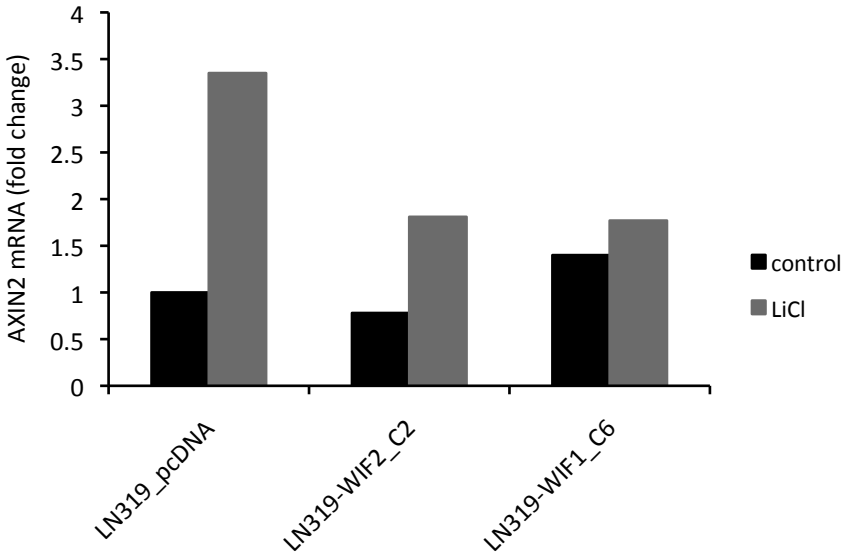


Fig. 7. Three clones have been treated with LiCl 30mM for 72 hours. mRNA has been analyzed with qPCR. All samples were normalized to LN319_pcDNA control. We could see AXIN2 levels increase after treatment. The biggest difference was seen in LN319_pcDNA, the only clone that doesn't express WIF1.

*WIF1 over-expressing cells adopt a senescence phenotype.*

Cell lines with ectopic expression of WIF1 previously showed a striking change in morphology once at confluence.[6] In addition to decreased growth rates, LN319-WIF1_C2 and LN319-WIF1_C6 showed enlarged size and flattened shape. We investigated recognized characteristics of senescence such as changes of ploidy, SA-ß-galactosidase activity and increased granularity.[29] As quantitative analysis, a fluorescent-activated cell sorting analysis (FACS) was performed. In FACS analysis, side scatter (SS) and forward scatter (FS) are used to identify cells. SS defines the cell granularity, FS defines the size. Senescent-like cell specifications were defined as: high granularity, high SS; big cell, high FS. A higher percentage of cells with such characteristics was found amongst WIF1-overexpressing clones in comparison with the control. In addition, this increased percentage was proportionally correlated with the respective expression of WIF1 of the different clones. The same observation was made after double staining of cells for SA-ß-galactosidase and DAPI, a DNA specific probe that stains the nucleus.[30] Higher populations of SA-ß-galactosidase positive and multi-nucleated cells were scored amongst both LN319- and LN229-derived WIF1-overexpressing clones [Fig 8].

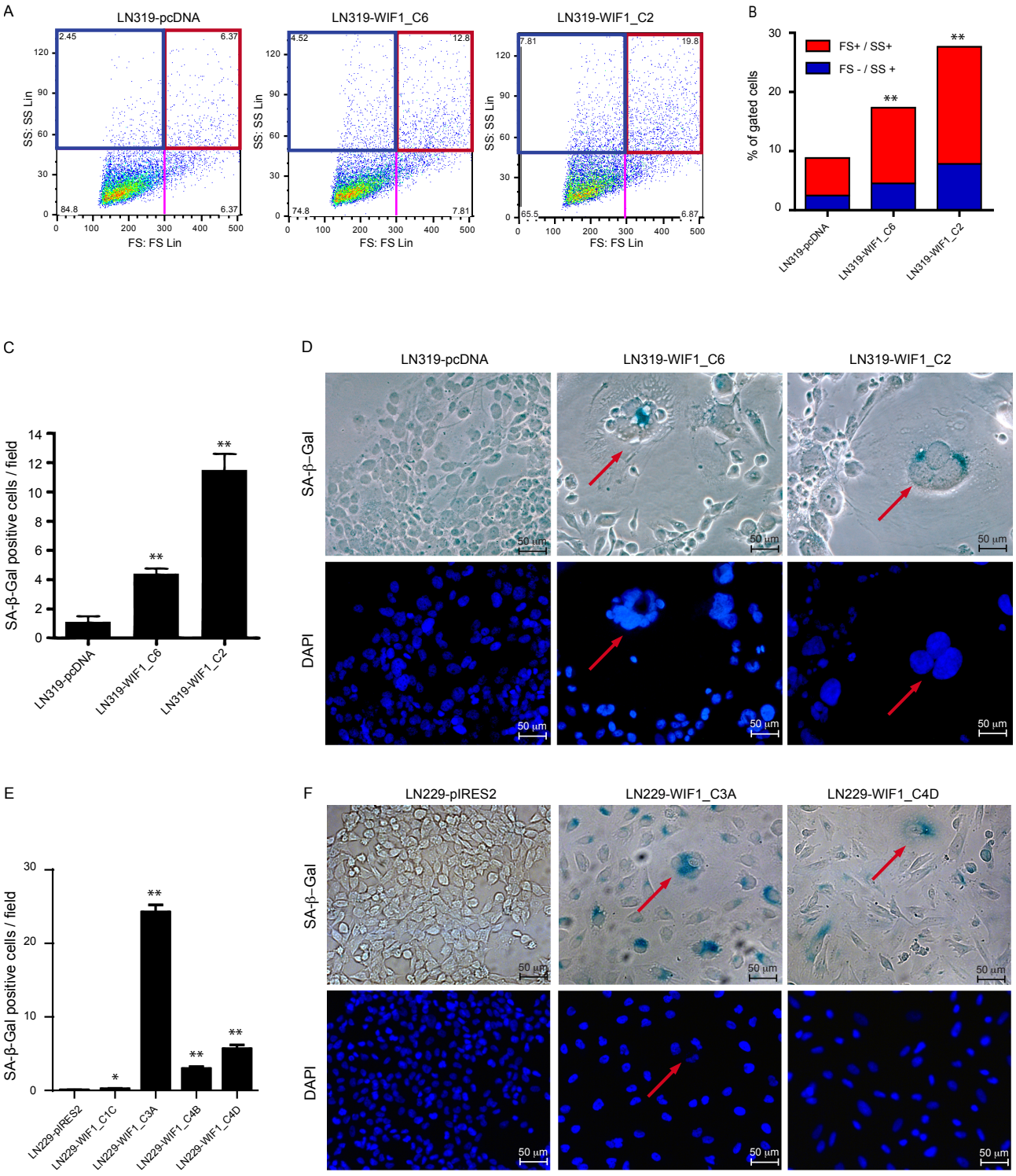


Fig. 8. WIF1 expression and detection of senescence-like cells. Cell morphology of the different LN319 clones was analyzed by fluorescence-activated cell sorting (FACS) (A). Senescence-like cells were defined as highly granulated cells, high side scatter (SS) (blue rectangle), and big cells, high forward scatter (FS) (red rectangle). (B) Quantification of FACS analysis, % of highly granulated cells (SS high, blue), and % of both highly granulated and big cells (FS and SS high, red). Quantification of LN319 (C) and LN229 (E) cells positive for SA-b-galactosidase activity scored in 10 different randomly chosen fields. (D, F) Representative images of clones stained for SA-b-galactosidase and DAPI are shown (200×). Large, SA-b-galactosidase positive (blue) and multi-nucleated cells are highlighted with red arrows. Results are marked with 1 asterisk (*) if P , .05 and 2 (**) if P , .01.[6]

*p21 seems not to play a role in WIF1-induced senescence-phenotype.*

LN319_pcDNA, LN319-WIF1_C2 and LN319-WIF1_C6 were tested for p21 and c-Myc expression. WIF1-overexpressing cells are sensitive to contact inhibition. All three clones were then taken in non-confluent state, defined as 60% of confluence, and confluent stage in order to distinguish between a fast- and slow-growing state. All data were analyzed using quantitative PCR and are thus reflecting the transcriptional regulation only.

Although p21 levels appeared to be higher in WIF1-overexpressing cell lines at the non-confluent stage, it is not the case at a confluent stage. In contrary, p21 levels are higher in the control than in both WIF1-overexpressing cell lines [Fig. 9A]. c-Myc levels are similar in all three clones at non-confluent stage. At confluent stage however, there is an increased c-Myc expression in the control but a decreased expression in the clones expressing WIF1 [Fig 9B].

A

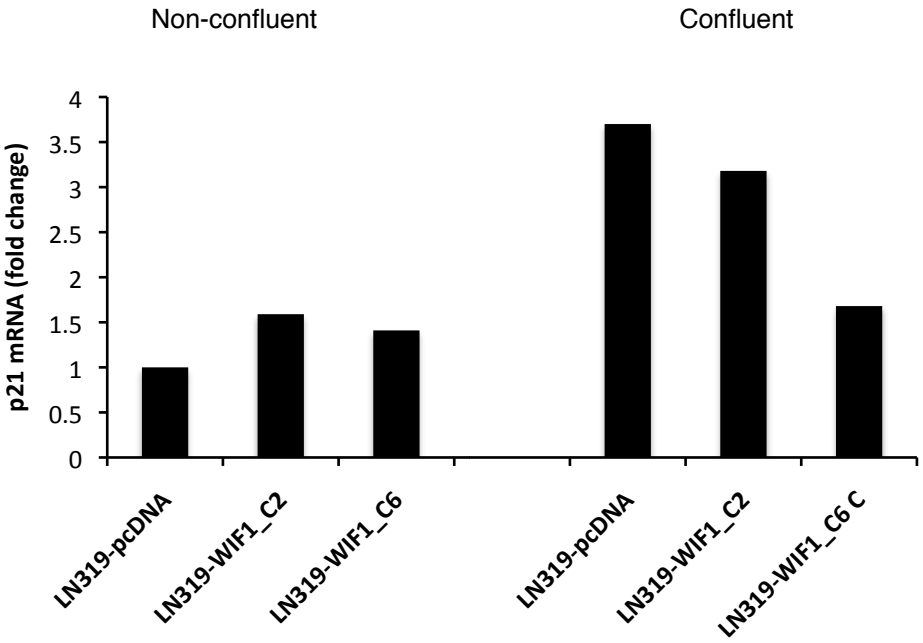

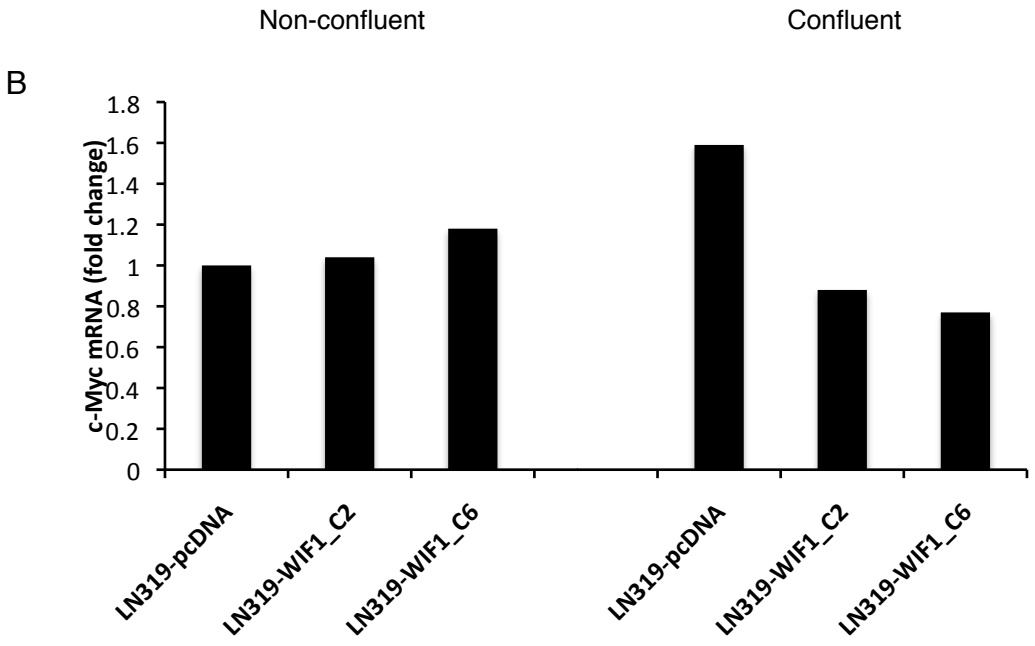


Fig. 9. The RNA of three clones was collected and analyzed with qPCR for p21 and c-Myc expression. All samples were normalized to LN319_pcDNA at confluent stage. (A) p21 levels of transcription appeared slightly higher in WIF1-overexpressing cells at a non-confluent stage. However it was the other way around at confluence. We think that other process are involved at this stage, more likely due to contact inhibition. (B) c-Myc levels are similar at non-confluent stage. At confluence however, the expression appeared to drop in WIF1-overexpressing cells. This could be explain by a higher concentration of WIF1 at confluent stage. However c-Myc and p21 expressions weren't correlated.

*Autophagy*

Amongst LN319 clones, IGFBP7 and especially ALDH1A3 were higher in the cells expressing WIF1, with a positive relationship to its level of expression [Fig. 10A]. We can observe some similarities to the quantitative analysis previously shown [Fig. 8A]. Expression of autophagy genes, on the other hand, was lower in those cells, exception made for ULK3 which was similar in all cell lines [Fig. 10B]. We found no indication of increased autophagy in WIF1-overexpressing cells. No clear relationship with WIF1 expression could be observed at this point.

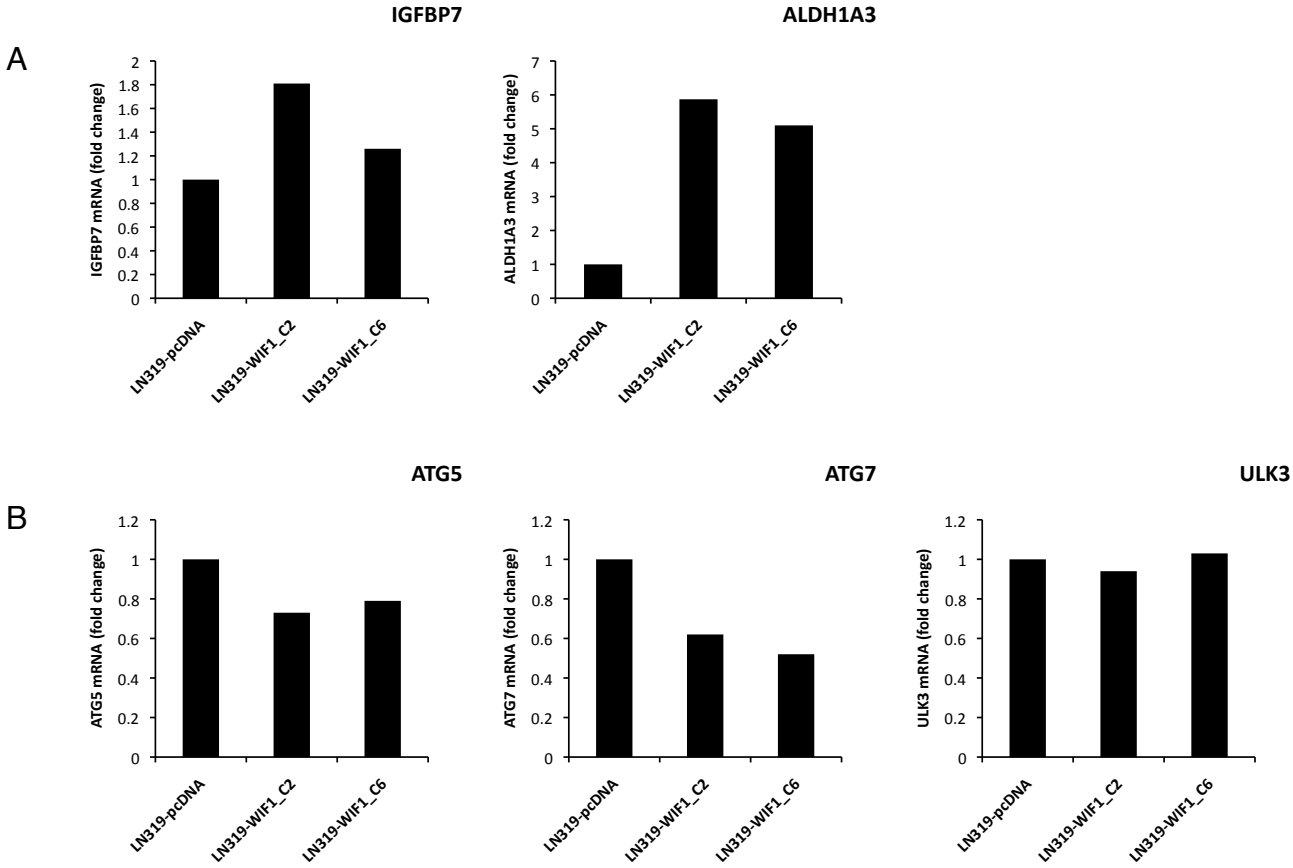


Fig. 10. LN319 clones mRNA was analyzed through qPCR for senescence and autophagy genes. (A) There was a increased expression of IGFBP7 and especially ALDH1A3 in WIF-overexpressing cell lines. We could observe a dose-dependent effect along with WIF1 expression (c.f. Fig 1). (B) ATG5 and ATG7 expression appeared lower in WIF1-overexpressing cell lines. ULK3 expression however stayed similar in all three cell lines. The relationship to WIF1 expression remains unclear at this point.

Amongst LN229 clones, IGFBP7 expression was higher in WIF1-overexpressing cells, with a strong relationship with WIF1 expression, as it can be observed in LN229-WIF1_C3A and LN229-WIF1_C4D, both clones with the highest WIF1 expression. ALDH1A3 expression showed a similar pattern, with higher expression in LN229-WIF1_C3A and LN229-WIF1_C4D but not in the other WIF1-expressing clones. In contrary, the expression appeared lower in these cells than in the control [Fig. 11A]. Interestingly, ATG5 and ATG7 expressions exerted the same pattern as IGFBP7 and ALDH1A3. They show strong expression in LN229-WIF1_C3A and LN229-WIF1_C4D which can be correlated to WIF1 expression [Fig. 11B]. ULK3 expression, however, correlated neither with WIF1 expression nor IGFBP7 or ALDH1A3 expression .

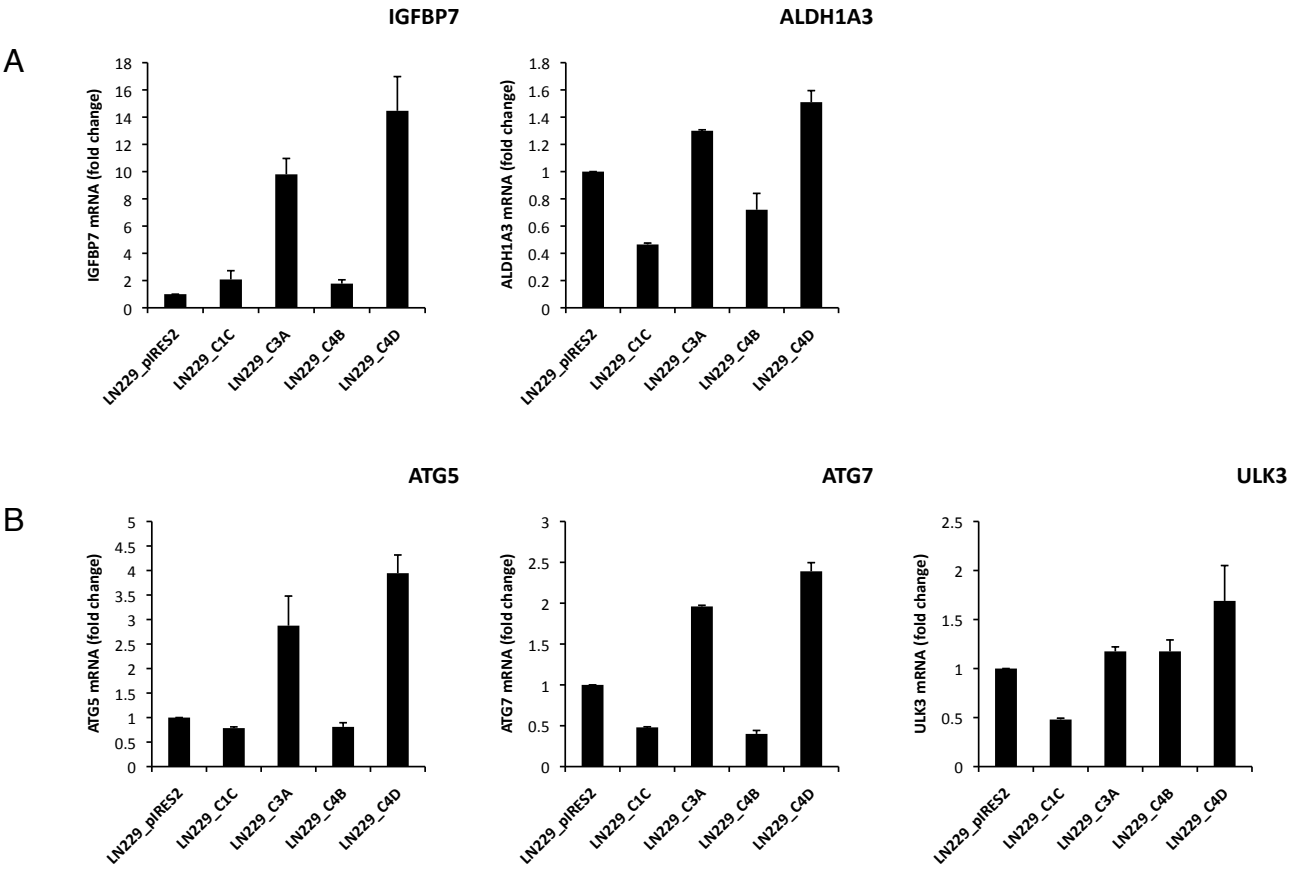


Fig. 11. LN229 clones mRNA was analyzed through qPCR for senescence and autophagy genes. (A) There is a strong increase in IGFBP7 expression in WIF-overexpressing cell lines. ALDH1A3 expression on the other hand didn't correlate with WIF1 expression in all clones. Nevertheless, the clones with the highest WIF1 expression, LN229_WIF1_C3A and LN229_WIF1_C4D showed an increased ALDH1A3 expression as expected (B) Interestingly, ATG5 and ATG7 expression showed a pattern similar to IGFBP7 and ALDH1A3. We observed a strong expression in LN229_WFI1_C3A and _C4D which matches WIF1 expression amongst these cell lines. ULK3 expression however could not be correlated to any other gene in those results.

# Discussion

By investigating specific markers and morphological characteristics, we have evidence for a senescence-like phenotype amongst WIF1-overexpressing cells. Moreover, we have established that this effect is due to WIF1 activity as it can be reversed using a Wnt-pathway activator like LiCl. These last results however can be criticized. The experiment has been performed only once. In addition, it does not explain why AXIN2 levels are higher in LN319_WIF1_C6 before treatment. In this cell line, Wnt signaling should be inhibited by WIF1, keeping AXIN2 expression at a lower level.

Nonetheless, our data confirms a certain role of Wnt-pathway in the tumorigenicity of glioblastoma, warranting further research in this particular signaling pathway. Moreover, it may also offer a target for new treatment strategies.
However, the intracellular process that leads to this state remains however unknown. p21 and c-Myc are key players in many neoplasiae, although no evidence of association between the expression of these genes and WIF1 expression could be found in our case. In order to be more certain of these results, our experiments should be repeated at least twice. The significantly increased expression of IGFBP7 and ALDH1A3 in LN319- and LN229-derived WIF1-overexpressing clones offers new tracks to explain the effect of WIF1 expression on the onset of senescence.

At this point, the role of autophagy in this process remains unclear. Autophagy related gene expression varies between the onsets of stress and senescence, as shown in human fibroblast.[13] It is possible that we missed the transition in our samples. We indeed did not analyze our samples at different time points. It is however interesting how similar ATG5 and ATG7 expressions are to ALDH1A3 and IGFBP7 in LN229-related WIF1-overexpressing cell lines. This can be a beginning in understanding the relationship between autophagy and senescence.

Further experiments are clearly required in order to firstly confirm these results and secondly investigate the potential association between the two processes. Does autophagy really mediate the onset of senescence, do they have a common trigger or is it just two patterns of the same process? The role of Wnt in autophagy activity stands as a challenge as well. Although a down-regulation of Wnt by autophagy itself has been described,[31] trigger of autophagy by Wnt inhibition has not been shown yet. A way to answer these questions is to create a WIF1 inducible system in GBM cell lines. By being able to control WIF1 expression in time, we would have the tool to investigate direct changes of expression at different time points. We would therefore be able to observe the transition into a senescent state, along with levels of autophagy activity. This system is currently being developed in the lab.

Glioblastoma is and remains a deadly disease, despite constant improvements in tumor management and the better resources we constantly develop to control it. It is therefore essential to further our knowledge and understanding of this devastating tumor in order to improve its poor prognosis. The new processes described above can potentially be a step

closer to a better prognosis, highlighting the importance of further observations and investigations in them.

# Acknowledgments

As a Master medical student, I want to clarify that I have just participated on the WIF1-project. The majority of the experiments were undertaken by Irene Vassallo, PhD Student in charge of the project. As it was my first experience in a lab, I had to learn basic procedures like cell-manipulation, -culture, -seeding and other protocols such as RNA extraction, retrotranscription, quantitative PCR and FACS analysis. It was with great help from Irene Vassallo that allowed me to undertake these procedures and to manage this project. I therefore deeply thank her for all the time she granted me.

I also thank Monika Hegi, PD, Head of Laboratory, for her supervision and her advice along the project.

Thanks to Annie-Claire Diserens, Marie-France Hamou, Davide Sciuscio, Maria Oikonomaki and Premnath Rajakannu for all their support and for the good moments we shared together.

## References


[1] Sant M, Minicozzi P, Lagorio S, Johannesen TB, Marcos-Gragera R, Francisci S. Survival of european patients with central nervous system tumors. Int J Cancer [Internet]. 2011 Jul 29 [cité 2011 Sep 5];Available from: http://www.ncbi.nlm.nih.gov/pubmed/21805473

[2] Ohgaki H, Kleihues P. Genetic profile of astrocytic and oligodendroglial gliomas. Brain Tumor Pathology. 2011 mars 26;28:177–83.

[3] Kleihues P, Ohgaki H. Primary and secondary glioblastomas: From concept to clinical diagnosis. Neuro-Oncology. 1999 Jan;1(1):44 -51.

[4] Stupp R, Hegi ME, Mason WP, van den Bent MJ, Taphoorn MJB, Janzer RC, et al. Effects of radiotherapy with concomitant and adjuvant temozolomide versus radiotherapy alone on survival in glioblastoma in a randomised phase III study: 5-year analysis of the EORTC-NCIC trial. Lancet Oncol. 2009 Mai;10(5): 459-466.

[5] Darefsky AS, King JT, Dubrow R. Adult glioblastoma multiforme survival in the temozolomide era: A population-based analysis of surveillance, epidemiology, and end results registries. Cancer. 2011;:n/a-n/a.

[6] Lambiv WL, Vassallo I, Delorenzi M, Shay T, Diserens A, Misra A, et al. The Wnt inhibitory factor 1 (WIF1) is targeted in glioblastoma and has a tumor suppressing function potentially by induction of senescence. Neuro-Oncology. 2011 Juillet 1;13(7):736 -747.

[7] Clevers H. Wnt/[beta]-Catenin Signaling in Development and Disease. Cell. 2006 Nov 3;127(3):469-480.

[8] Rebecca Henretta, Laboratory Investigation, advance online publication. 8 January 2007; doi:10.1038/labinvest.3700509

[9] Foltz G, Yoon J, Lee H, Ma L, Tian Q, Hood L, et al. Epigenetic Regulation of Wnt Pathway Antagonists in Human Glioblastoma Multiforme. Genes Cancer. 2010 Jan;1(1):81-90.

[10] Yang Z, Wang Y, Fang J, Chen F, Liu J, Wu J, et al. Expression and aberrant promoter methylation of Wnt inhibitory factor-1 in human astrocytomas. J. Exp. Clin. Cancer Res. 2010;29:26.

[11] Yang Z, Wang Y, Fang J, Chen F, Liu J, Wu J, et al. Downregulation of WIF-1 by hypermethylation in astrocytomas. Acta biochimica et biophysica Sinica. 2010;42(6):418.

[12] Gartel AL, Ye X, Goufman E, Shianov P, Hay N, Najmabadi F, et al. Myc represses the p21(WAF1/CIP1) promoter and interacts with Sp1/Sp3. Proc Natl Acad Sci U S A. 2001 avr 10;98(8):4510–5.

[13] Young AR, Narita M, Ferreira M, Kirschner K, Sadaie M, Darot JF, et al. Autophagy mediates the mitotic senescence transition. Genes Dev. 2009 Avr 1;23(7):798-803.

[14] Cecconi F, Levine B. The Role of Autophagy in Mammalian Development. Dev Cell. 2008 sept;15(3):344–57.

[15] Mizushima N, Levine B, Cuervo AM, Klionsky DJ. Autophagy fights disease through cellular self-digestion. Nature. 2008 Fév 28;451(7182):1069-1075.

[16] Cell Signaling Technology, Inc. Image. [Internet]. September 2007 [November 2010]. Available from: <http://www.cellsignal.com/reference/pathway/Autophagy.html>

[17] Levine B, Kroemer G. Autophagy in the Pathogenesis of Disease. Cell. 2008 janv 11;132(1):27–42.

[18] Young AR, Narita M. Connecting autophagy to senescence in pathophysiology. Curr. Opin. Cell Biol. 2010 Avr;22(2):234-240.

[19] Fridman AL, Tainsky MA. Critical pathways in cellular senescence and immortalization revealed by gene expression profiling. Oncogene. 2008 online;27(46):5975–87.

[20] Ishii N, Maier D, Merlo A, et al. Frequent co-alterations of TP53, p16/ CDKN2A, p14ARF, PTEN tumor suppressor genes in human glioma cell lines. Brain Pathol. 1999;9(3):469 – 479.

[21] Lorenzi PL, Reinhold WC, Varma S, et al. DNA fingerprinting of the NCI-60 cell line panel. Mol Cancer Ther. 2009;8(4):713–724.

[22] Chan SL, Cui Y, van Hasselt A, et al. The tumor suppressor Wnt inhibi- tory factor 1 is frequently methylated in nasopharyngeal and esopha- geal carcinomas. Lab Invest. 2007;87(7):644 – 650.

[23] Andreeff M, Ruvolo V, Gadgil S, et al. HOX expression patterns identify a common signature for favorable AML. Leukemia. 2008;22(11): 2041 – 2047.

[24] Lal M, Song X, Pluznick JL, et al. Polycystin-1 C-terminal tail associates with beta-catenin and inhibits canonical Wnt signaling. Hum Mol Genet. 2008;17(20):3105 – 3117.

[25] Sidi R, Pasello G, Opitz I, Soltermann A, Tutic M, Rehrauer H, et al. Induction of senescence markers after neo-adjuvant chemotherapy of malignant pleural mesothelioma and association with clinical outcome: An exploratory analysis. European Journal of Cancer. 2011 1;47(2):326-332.

[26] Klein PS, Melton DA. A molecular mechanism for the effect of lithium on development. Proc Natl Acad Sci U S A. 1996 août 6;93(16):8455–9.

[27] O'Brien WT, Harper AD, Jove F, Woodgett JR, Maretto S, Piccolo S, et al. Glycogen synthase kinase-3beta haploinsufficiency mimics the behavioral and molecular effects of lithium. Journal of Neuroscience. 2004;24(30):6791–8.

[28] Jho E-hoon, Zhang T, Domon C, Joo C-K, Freund J-N, Costantini F. Wnt/{beta}-Catenin/Tcf Signaling Induces the Transcription of Axin2, a Negative Regulator of the Signaling Pathway. Mol. Cell. Biol. 2002 févr 15;22(4):1172–83.

[29] Chang B-D, Broude EV, Dokmanovic M, Zhu H, Ruth A, Xuan Y, et al. A Senescence-like Phenotype Distinguishes Tumor Cells That Undergo Terminal Proliferation Arrest after Exposure to Anticancer Agents. Cancer Research. 1999;59(15):3761–7.

[30] Kapuscinski J. DAPI: a DNA-specific fluorescent probe. Biotech Histochem. 1995 sept;70(5):220–33.

[31] Gao C, Cao W, Bao L, Zuo W, Xie G, Cai T, et al. Autophagy negatively regulates Wnt signalling by promoting Dishevelled degradation. Nat Cell Biol. 2010;12(8):781–90.

*Neuro-Oncology* 13(7):736–747, 2011.
doi:10.1093/neuonc/nor036
Advance Access publication June 3, 2011



# The Wnt inhibitory factor 1 (WIF1) is targeted in glioblastoma and has a tumor suppressing function potentially by induction of senescence

Wanyu L. Lambiv†, Irene Vassallo†, Mauro Delorenzi, Tal Shay, Annie-Claire Diserens, Anjan Misra, Burt Feuerstein, Anastasia Murat, Eugenia Migliavacca, Marie-France Hamou, Davide Sciuscio, Raphael Burger, Eytan Domany, Roger Stupp, and Monika E. Hegi

*Laboratory of Brain Tumor Biology and Genetics (W.L.L, I.V., A-C.D., A.M., M-F.H., D.S., R.B., M.E.H.), Neurosurgery, Lausanne University Hospital and University of Lausanne, Lausanne (W.L.L., I.V., A-C.D., A.M., M-F.H., D.S., R.B., M.E.H., R.S.); Swiss Institute for Bioinformatics (M.D., E.M) and National Center of Competence in Research (NCCR) Molecular Oncology, ISREC EPFL-SV (M.D., E.M., M.E.H.); Department of Physics of Complex Systems, Weizmann Institute of Science, Rehovot Israel (T.S., E.D.); Department of Neurology, Barrow Neurological Institute St. Joseph's Hospital and Medical Center, Phoenix, AZ (A.M., B.F.)*

**Gene expression—based prediction of genomic copy number aberrations in the chromosomal region 12q13 to 12q15 that is flanked by *MDM2* and *CDK4* identified Wnt inhibitory factor 1 (*WIF1*) as a candidate tumor suppressor gene in glioblastoma. *WIF1* encodes a secreted Wnt antagonist and was strongly downregulated in most glioblastomas as compared with normal brain, implying deregulation of Wnt signaling, which is associated with cancer. *WIF1* silencing was mediated by deletion (7/69, 10%) or epigenetic silencing by promoter hypermethylation (29/110, 26%). Co-amplification of *MDM2* and *CDK4* that is present in 10% of glioblastomas was associated in most cases with deletion of the whole genomic region enclosed, including the *WIF1* locus. This interesting pathogenetic constellation targets the RB and p53 tumor suppressor pathways in tandem, while simultaneously activating oncogenic Wnt signaling.**

**Ectopic expression of *WIF1* in glioblastoma cell lines revealed a dose-dependent decrease of Wnt pathway activity. Furthermore, *WIF1* expression inhibited cell proliferation in vitro, reduced anchorage-independent growth in soft agar, and completely abolished tumorigenicity in vivo. Interestingly, *WIF1* overexpression in glioblastoma cells induced a senescence-like phenotype that was dose dependent. These results provide evidence that WIF1 has tumor suppressing properties. Downregulation of *WIF1* in 75% of glioblastomas indicates frequent involvement of aberrant Wnt signaling and, hence, may render glioblastomas sensitive to inhibitors of Wnt signaling, potentially by diverting the tumor cells into a senescence-like state.**

**Keywords:** epigenetic silencing, glioblastoma, senescence, tumor suppressor gene, WIF1, Wnt pathway.

Glioblastoma is the most malignant primary brain tumor with a median survival of only 15 months despite modern therapy comprising surgical resection followed by combined radiochemotherapy.[1] Thus new avenues need to be explored. High-throughput genomic data derived from human glioblastomas are readily available for analyses aiming at uncovering hitherto unrecognized disease mechanisms suitable as drugable targets, or identifying biomarkers for response to therapy. However, extracting relevant and reliable information from such data is not trivial.[2] Target gene identification in tumor tissue is often

Received August 27, 2010; accepted March 9, 2011.

†These two authors contributed equally to the present report.

**Corresponding Author:** Monika E. Hegi, Laboratory of Brain Tumor Biology and Genetics, Department of Neurosurgery, Lausanne University Hospital (CHUV BH19-110), 46, rue du Bugnon, Lausanne 1011, Switzerland (monika.hegi@chuv.ch)

complicated by (1) broad genomic copy number aberrations (CNAs), (2) multiple mechanisms of activating and inactivating genetic and epigenetic alterations, and (3) the complexity of pathway regulation. Further, the measurements may be confounded by contaminating nontumoral cells or the molecular heterogeneity of the tumor. Thus hidden tumor characteristics may only be unveiled with a multidimensional approach.[3,4]

Here we aimed at identifying and validating functionally new candidate genes relevant for the malignant behavior of glioblastoma. Since gene expression reflects both gene dosage effects by genomic CNAs and epigenetic modulation, we interrogated gene expression profiles derived from glioblastomas of patients treated within clinical trials[5–7] to infer underlying molecular changes. In the present study we focused on the chromosomal region on chromosome 12 (12q13 to 12q15) flanked by *MDM2* and *CDK4* that are known to be co-amplified in approximately 10% of glioblastomas, while the region in between is generally not amplified,[8] hence potentially indicating the presence of a tumor suppressor gene.

Indeed, by combining gene expression data with data from genomic copy number analysis, we identified Wnt inhibitory factor 1 (*WIF1*) as a new candidate tumor suppressor gene involved in glioblastoma. This gene encodes a secreted Wnt antagonist sequestering secreted Wnt proteins[9,10] and is thus predestined as a candidate tumor suppressor. The interaction of WIF1 with Wnt ligands blocks their binding with the cell surface cognate receptor downregulating activation of the pathway. Hence, loss of WIF1 expression is expected to aberrantly activate Wnt signaling, which is associated with cancer. CpG island hypermethylation of the *WIF1* promoter as silencing mechanism has been described in several epithelial cancers[11,12] and more recently also in glioma where it seems to be associated with tumor grade.[13]

Here we are reporting the tumor suppressing properties of WIF1 in in vitro and in vivo models of glioblastoma and propose a mechanism of action.

## Materials and Methods

### *Glioblastoma Tissues*

Glioblastoma tissues were collected for translational research with informed consent of the patients. The protocols were approved by the local ethics committees.

### *Prediction of Genomic Copy Number Amplifications in Glioblastoma by a Hidden Markov Model*

The glioblastoma micro-array gene expression data obtained in our laboratory on Affymetrix HG-133 Plus2.0 GeneChips (Gene Expression Omnibus database at http://www.ncbi.nlm.nih.gov/geo/, accession number GSE7696)[5] were used for amplification prediction. Probe sets were filtered to exclude those with low variance, suggestive of no or constant expression of the gene. For each gene with multiple probe sets, only the one with the highest variance was retained. Input to a hidden Markov model (HMM) as observed sequences were genewise-mean-centered, the log-scale robust multi-array average normalized expression data ordered by their positions on a chromosome (http://genome.ucsc.edu/; 2004 freeze) and discretized into 8 levels of expression intensity. The HMM had 2 hidden states: The "normal" state modeled the typical distribution, while the "activated" state modeled a distribution typical for highly amplified regions, which is shifted toward higher values. It generated for each sample and chromosome a matrix of posterior state probabilities at each of the measured loci.

### *HMM Training*

The emission probabilities of the HMM were based on frequencies of the discrete levels of expression as estimated from gene expression data for all genes from a large breast cancer sample population profiled with Affymetrix U133A chips ("normal" state) respectively from data subsets for genes in regions around the *ERBB2* gene that by statistical examination of the gene expression data were considered amplified ("activated" state). A dozen of these calls were tested by reverse transcription PCR and the status of all those tested was confirmed. High posterior probabilities for the activated state are obtained for probe sets in regions where amplifications or another cause results in higher average expression of contiguous genes. In breast cancer and in glioblastoma, the method identified primarily activated regions known from the literature to be subjected to high degree amplifications (unpublished observation). Transition probabilities were estimated so that a posterior probability of 0.5 was a useful cutoff to identify amplified regions. Posterior state probabilities were computed using the Markov Modeling Tool (MAMOT) program[14] with a manually curated model parameter file.

### *DNA Isolation, Methylation-Specific PCR*

Genomic DNA was isolated from paraffin-embedded or fresh frozen tissue and subjected to bisulfite treatment using the EZ DNA Methylation Kit (Zymo Research) followed by nested methylation-specific PCR (MSP), as described previously.[15] During the bisulfite treatment, unmethylated cytosine, but not its methylated counterpart, is converted into uracil. MSP for *WIF1* was performed via a nested approach using published primer sequences.[12] Peripheral blood lymphocytes and the colon cancer cell line SW48 were employed as the *WIF1* methylation negative and positive controls, respectively.

### *RNA Isolation and Reverse Transcription PCR*

Total RNA was extracted using the RNeasy total RNA extraction kit (Qiagen), and cDNA was synthesized

using Superscript RT II (Invitrogen). PCR was performed with gene-specific primers for *WIF1*.[12] *POLR2A* expression was assayed to control for mRNA integrity using published primers.[16] Real-time quantitative PCR was performed with Fast SybR Green Master Mix (Applied Biosystem) using the Rotor Gene 6000 Real-Time PCR system (Corbett Life Science). PCR reactions were run as triplicates. The temperature profile was as follows: 95°C (100 s) followed by 40 cycles at 95°C (3 s) to 60°C (20 s). The quality of the products was controlled by the melting curve. Transcript levels were normalized against human *GAPDH*.[17] *WIF1* primers: Forward: 5′-AAGGTTGGCATGGAAG ACAC-3′; Reverse: 5′- TTAAGTGAAGGCGTGTGCTG -3′. *AXIN2* primers.[18]

### *Glioblastoma Cell Lines*

Glioblastoma cell lines LN18, LN229, LN235, LN319, LN401, LN992 were established in our lab, and U87MG was obtained from the American Type Culture Collection (ATCC). All glioma cell lines have been characterized for a defined set of molecular aberrations in our lab, as published previously,[19] and were controlled by DNA fingerprinting as described.[20] The non–small cell lung carcinoma cell line A549 and the colon carcinoma cell line SW48 were obtained from ATCC. All lines were cultured in Dulbecco's modified Eagle's medium (Invitrogen), supplemented with 5% fetal calf serum (Hyclone) and 100 units/mL penicillin, 100 units/mL streptomycin (Invitrogen). For global demethylation of DNA, glioblastoma cell lines were treated with 5 μM 5-aza-2′-deoxycytidine (Sigma-Aldrich Chemie) for 96 h, with 24-h medium renewal.[21]

### *Plasmids and Small Interference RNAs*

The Wnt/β-catenin activity luciferase reporter vectors TOP5 and FOP5 comprise T-cell factor (TCF)/β-catenin responsive elements that express synthetic firefly luciferase from a PGL4.10 backbone with a minimal TATA box with 5 concatenated TCF binding sites and 5 mutated binding sites, respectively (a generous gift of Dr M. van de Wetering).[22] The pRL CMV Renilla luciferase (Promega AG) plasmid was used to normalize for transfection efficiency. The *WIF1* expression vector and its empty control pcDNA3.1 vector were generous gifts from Professor Qian Tao, Cancer Center, Chinese University of Hong Kong.[23] To generate the stably transfected clones in the LN229 cell line, *WIF1* was subcloned into the vector pIRES2-EGFP (Clontec). *WIF1* knockdown was achieved using small interference RNAs (siRNAs; ON-TARGET plus SMART pool, Dharmacon RNA Technologies) targeting 3 domains of the *WIF1* RNA, and the control experiments were performed with the corresponding ON-TARGET plus nontargeting pool.

### *Transfection and Dual Luciferase Assay*

For transient transfections, cells were grown to 80% confluence in 24-well plates. Transfections were performed with Lipofectamine 2000 transfection reagent (Invitrogen), and siRNAs were transfected with INTERFERin (Polyplus-Transfection SA) reagent as suggested by the manufacturers.

For Wnt pathway activity reporter assays, cells were transfected with 0.25 μg of either of TOP5 or FOP5 and 5 ng of Renilla pRL CMV luciferase construct, and incubated at 37°C for 28 h. Subsequently the firefly and Renilla luciferase activities were measured using Dual-Luciferase Reporter assay reagents (Promega). The Renilla luciferase activity was used to normalize for transfection efficiency. The Wnt pathway-specific activity status was determined by the TOP5/FOP5 ratio. A TOP5/FOP5 ratio significantly higher than 1 was considered as an active Wnt pathway. The cell line A549 served as positive control.[24] These experiments were performed in triplicate and were replicated 2 or 3 times independently. Modulation of the Wnt pathway in established cell lines was effectuated by cotransfection of corresponding plasmids or siRNAs. In these experiments, Wnt pathway activation status was assessed 72 h post transfection. For stable transfections, cells were transfected either with the *WIF1* expression vector or a control vector followed by selection with G418. Resistant clones were selected and maintained in 400 μg/mL of G418.

### *Crystal Violet Assay*

For growth curves, $1 \times 10^4$ cells were seeded in 24-well plates. At every time point, culture medium was removed, cells were washed with 1 mL of 1.0× phosphate buffered saline (PBS), and 300 μL of crystal violet solution was added per well. After 10 min at 37°C, crystal violet solution was removed and plates were washed with 1× PBS. Plates were left to dry overnight, and 500 μL of 1% sodium dodecyl sulfate in distilled water was added per well. Absorbance was then measured at 595 nm using a plate reader.

### *Enzyme-Linked Immunosorbent Assay*

The cell supernatant, collected after 2 days of culture, was quantified for secreted WIF1 with a sandwich enzyme-linked immunosorbent assay (R&D System) following the manufacturer's instructions. Data were normalized to the cell number. For control experiments of small interfering WIF1 efficiency, the medium was collected after 3 days of culture, and data were normalized to protein content.

### *Colony Formation Assay in Soft Agar*

Growth in soft agar was determined in 6-well plates containing 2 mL of 1% agar in complete medium as the bottom layer, and 1 mL of 0.4% agar in complete

medium as the top layer. Cells, $1 \times 10^4$ and $2 \times 10^3$, respectively, were seeded in triplicate. Cultures were maintained under standard conditions, and after 3 weeks the number of colonies was determined with an inverted phase-contrast microscope, where a group of >50 cells was scored as colony.

### *Nude Mouse Tumorigenicity Assay*

Cells ($7 \times 10^6$) were resuspended in Dulbecco's modified Eagle's medium and subcutaneously injected into the flanks of 6- to 9-week-old female Swiss nu/nu mice. Five mice per group were injected, and tumor size was measured weekly with a caliper. Tumor volume ($mm^3$) was calculated as (length × width$^2$)/2. The protocol was authorized by the local veterinary authorities (VD1181-3).

### *Flow Cytometry Measurement of Cell Morphology*

Cells were grown until confluence detached using a solution of 2 mM ethylenediaminetetraacetic acid in PBS and resuspended in PBS. Cell size was evaluated by forward scatter (FS) and side scatter (SS) analysis using a Beckman Coulter FC500 5-color analyzer. More than $1 \times 10^4$ events were counted for all samples. Thresholds for FS and SS were arbitrarily defined.

### *Histochemistry*

Cells were seeded onto glass coverslips coated with poly-L-lysine and cultured until confluence. Cells were stained for the activity of SA-β-galactosidase using the β-Galactosidase Staining Kit (Biovision), following the manufacturer's instructions, and counterstained with 4′,6-diamidino-2-phenylindole (DAPI). SA-β-galactosidase activity and nuclear morphology were visualized by bright field and fluorescence microscopy (Leica Leitz DMRB). Cells were scored in 10 randomly taken fields.

## Results

### *Gene Expression–Based Prediction*

Gene expression profiles obtained in our lab from 80 human glioblastoma samples[5] were used to infer underlying molecular alterations. Inspection of the chromosomal region encompassing *CDK4* and *MDM2* using an HMM predicted separate amplifications of these proto-oncogenes (Fig. 1A), that is, no co-amplification comprising the genomic region in between. Although this 2-state HMM was not constructed to detect deleted loci, we had indications of several loci with very low average and low maximum posterior probability for the activated state, thus pointing to loci potentially targeted for expression silencing. The array comparative genomic hybridization (aCGH) data of this cohort (Shay and Lambiv, manuscript in preparation) confirmed the amplifications and indicated deleted loci at positions of low amplification probability (Fig. 1B). The deleted locus in proximity to *CDK4* was queried by a single Bacterial Artificial Chromosome (BAC) probe (RP11-97A6) in the aCGH data and was scored as deleted in 16 of 55 glioblastomas (29%). The minimal deleted locus in proximity to *MDM2* affected 2 BACs (RP11-109L8 and RP11-18B8), spanning approximately 1.5 Mb and encompassing 6 known genes (*WIF1*, *LEMD3*, *MSRB3*, *HMGA2*, *IRAK3*, and *HELB*) (http://genome.ucsc.edu/; 2004 freeze, hg17). Deletion of this locus affected 7 of 69 (10%) glioblastomas. Of note, most samples with co-amplification of *MDM2* and *CDK4* exhibited a deletion of the genomic region between these 2 loci, suggesting a merged amplicon (Fig. 1C). Hence, this interesting pathogenetic constellation combines amplification of 2 oncogenes plus deletion of putative tumor suppressor genes in a single event. This CNA pattern was confirmed in the database of The Cancer Genome Atlas (TCGA)[25] (Supplementary Fig. S1). Among the potential candidate target genes, *WIF1* showed the largest mRNA expression variation in this data set, and median *WIF1* expression was significantly lower in glioblastoma than in 4 nonneoplastic brain tissues ($P = .001$, 2-sample Wilcoxon test) (Fig. 1D). The other genes exerted expression levels similar to those of normal brain tissue and/or showed relatively low variation in our data set. The low expression of *WIF1* in glioblastoma was confirmed in all 5 independent glioblastoma data sets analyzed[26–30] (Fig. 1E). Furthermore, decreasing expression of *WIF1* is associated with tumor grade in astrocytoma, as suggested by 2 independent data sets.[31,32] *WIF1* encodes a soluble Wnt pathway antagonist sequestering Wnt proteins, thereby inhibiting their function.[9] Since Wnt signaling is proto-oncogenic,[33] modulators/antagonists of Wnt signaling are good candidates for tumor suppressor functions.[34]

### *WIF1 is Silenced Both by Genomic Deletion and Promoter Hypermethylation*

While expression data suggested low *WIF1* expression in 76% of glioblastomas of our gene expression data set, corresponding analysis of the aCGH data showed hemizygous deletions at the *WIF1* locus in only 10% (7/69), suggesting other mechanisms of silencing. Subsequent analysis of the *WIF1* promoter by MSP revealed hypermethylation in 2 of 6 glioblastomas with hemizygous deletion, satisfying the 2-hit model of tumor suppressors. In an extended series of 110 glioblastomas, 26% exerted a methylated *WIF1* promoter (Fig. 2). *WIF1* mutations have not been reported from glioblastoma (0/444), according to the Catalogue of Somatic Mutations in Cancer (COSMIC) database.[35]

Interestingly, a significant association with methylation of the O6-methylguanine DNA-methyltransferase (*MGMT*) promoter was observed ($P = .004$, 2-sided Fisher exact test). *MGMT* methylation is a known predictive factor for response to alkylating agent therapy

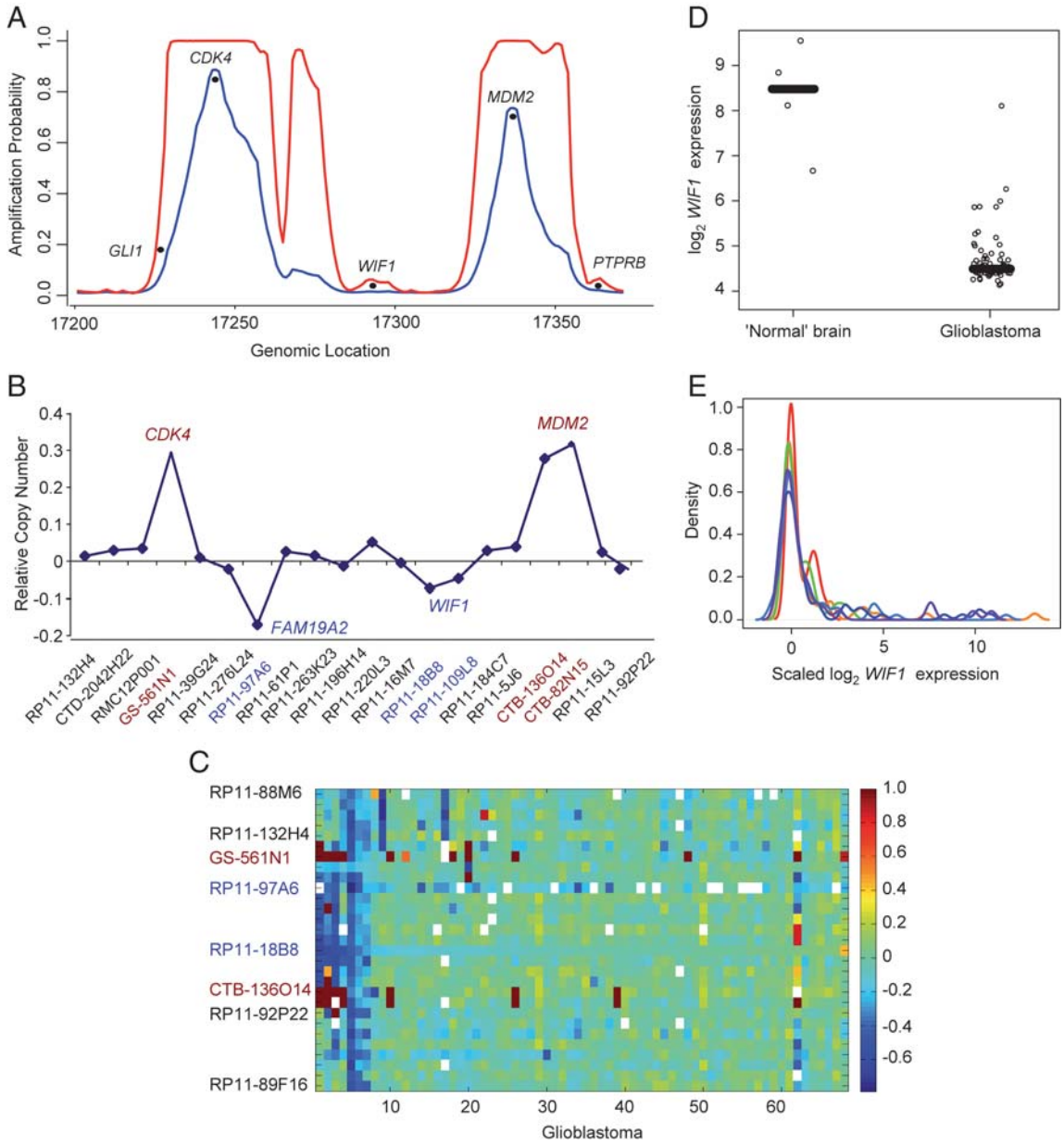


Fig. 1. Gene expression–based prediction of copy number aberrations (CNAs) in glioblastoma. (A) The maximum (red) and mean (blue) amplification probabilities on chromosome 12q14–12q15 were estimated from glioblastoma gene expression data by a hidden Markov model (HMM). The interrogated region flanked by *CDK4* and *MDM2* encompasses a ~11 Mb window. (B) The respective mean DNA copy number of this chromosomal region was determined by array comparative genomic hybridization (aCGH, Humarray 3.0 and 3.1 of the University of California at San Francisco; manuscript in preparation). The bacterial artificial chromosome (BAC) probes are ordered by their genomic positions. The BACs corresponding to *CDK4* and *MDM2* BACs are shown in red. (C) The heat map visualizes the structure of the aCGH data shown in (B) for the genomic region encompassing 12q13 to 12q15 from 68 glioblastomas. The BACs are ordered by their genomic position, while the glioblastomas on the *x*-axis are ordered by similarity using Sorting Points into Neighborhood software.[57] Blue depicts deletion; red, amplification; and white, missing data. The color scale is truncated to [−1, 1] for presentation. The BAC corresponding to *CDK4* is GS-561N1; for *MDM2,* CTB-136O14 (red); and for *WIF1,* RP11-18B8 (blue). (D) *WIF1* expression (Affymetrix probe set 204712_at) in glioblastoma is significantly lower than in nonneoplastic brain tissues ($P = .001$), as determined in our gene expression data set.[5] (E) Low *WIF1* expression was confirmed in 5 independent glioblastoma data sets (Freije *et al.*, red; Rich *et al.*, violet; Phillips *et al.*, orange; Sun *et al.*, dark blue; Horvath *et al.*, green; our data set, Murat *et al.*, light blue).[26–30] *WIF1* expression values are median centered within each data set independently.

in glioblastoma.[15,36] The *MGMT* methylation status was available for 107 cases from previous studies, of which 56 were *MGMT* methylated (52%).[5,37–40] Most established glioblastoma cell lines (14 of 15) showed hypermethylation of the *WIF1* promoter. Only LN992 exhibited an unmethylated *WIF1* promoter. Treatment

of glioblastoma cell lines with the DNA demethylating agent 5-aza-cytidine for 96 h restored *WIF1* expression (Fig. 3A).

### *Modulation of WIF1 Expression Affects Wnt Pathway Activation*

Wnt pathway activity was tested in a set of 7 glioblastoma cell lines using the TOP5/FOP5 Wnt signaling reporter system that investigates transactivation of the TCF responsive element (5 concatenated TCF binding sites) normalized to transactivation of the corresponding mutated binding sites (5 concatenated mutated TCF binding sites). Wnt pathway activity was present in all cell lines with low or no detectable *WIF1* expression, while LN235 and LN992 showed no significant Wnt activity (TOP5/FOP5 $\leq 1$), in accordance with high levels of endogenous *WIF1* expression (Fig. 3A and B). Given the role of WIF1 in regulation of Wnt signaling, and the prevalence of low *WIF1* expression in glioblastoma, we first investigated the glioblastoma cell lines with endogenous Wnt pathway activity and asked if *WIF1* overexpression translates into impaired Wnt signaling. Indeed, forced expression of *WIF1* inhibited Wnt activity in a dose-dependent manner (Fig. 3C). Next we examined whether in the 2 cell lines with endogenous *WIF1* expression and no Wnt signaling activity (LN992 and LN235, Fig. 3A and B) the pathway could be activated upon *WIF1* silencing. Using siRNA to knock down *WIF1* expression, we detected induction of Wnt signaling activity in both cell lines, in contrast to the controls with nontargeting siRNAs (Fig. 3D, Supplementary Fig. S2).

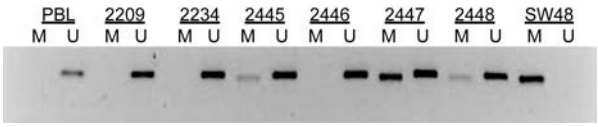


Fig. 2. Promoter methylation of *WIF1* in glioblastoma. Methylation-specific PCR (MSP) for *WIF1* was performed via a nested approach using published primer sequences.[12] DNA isolated from peripheral blood lymphocytes (PBLs) and the colon cancer cell line SW48 served as controls for unmethylated (U) and methylated (M) *WIF1* promoter status, respectively. Glioblastomas #2445, #2447, and #2448 contain a methylated *WIF1* promoter, whereas the others harbor only an unmethylated gene promoter.

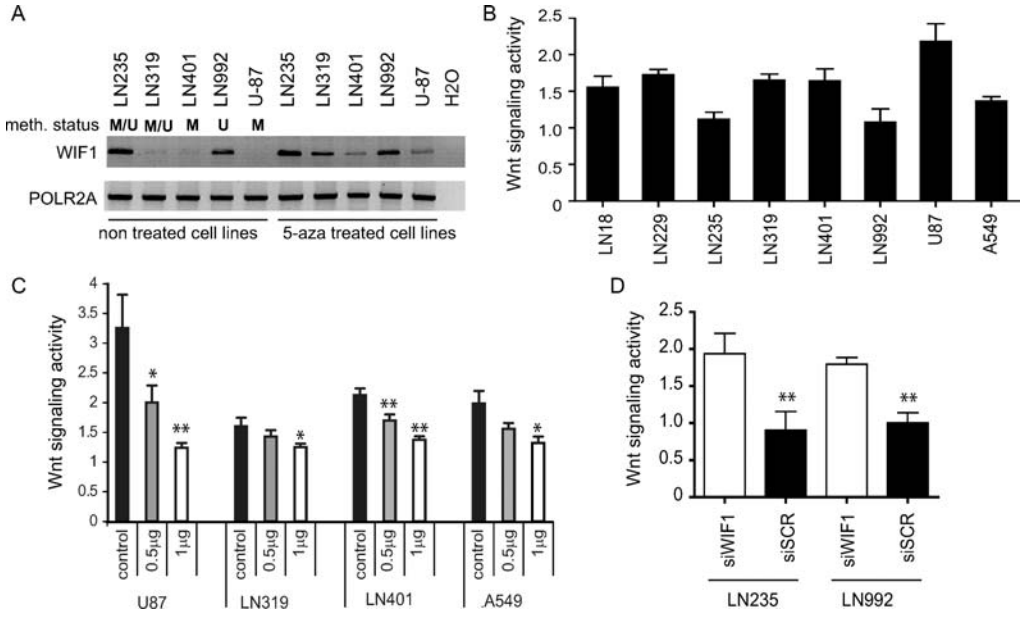


Fig. 3. Alteration of *WIF1* expression modulates Wnt signaling. (A) Glioblastoma cell lines were treated with the DNA demethylating agent 5-aza-cytidine for 4 days. All 3 *WIF1* nonexpressing cell lines with a methylated *WIF1* promoter re-expressed *WIF1* mRNA in response to 5-aza-cytidine treatment (LN319, LN401, U87). Only LN992 was completely unmethylated. The lower panel shows mRNA expression of the *POLR2A* gene used to control for mRNA quality. The methylation status of the cell lines displayed was determined by MSP. (B) Wnt signaling activity was measured with the TCF luciferase reporter (TOP5/FOP5; ratio >1 Wnt pathway active). The non–small cell lung carcinoma cell line A549 served as positive control. LN235 and LN992 show no significant activity. (C) Wnt signaling (TOP5/FOP5) after cotransfection of increasing amounts (0 µg, 0.5 µg, and 1 µg) of the *WIF1* expression vector into glioblastoma cell lines U87, LN319, LN401, and A549. The DNA quantity was adjusted with the control vector. (D). LN235 and LN992, negative for Wnt signaling activity, were transfected with si*WIF1* and the siScrambled as control. Knockdown of *WIF1* induced Wnt pathway activity (TOP5/FOP5) in both LN992 and LN235. *WIF1* expression measured after transfection of *siWIF1* or the respective control siRNAs is documented in Supplementary Fig. S2. Results are marked with 1 asterisk (*) if $P < .05$ and 2 (**) if $P < .01$.

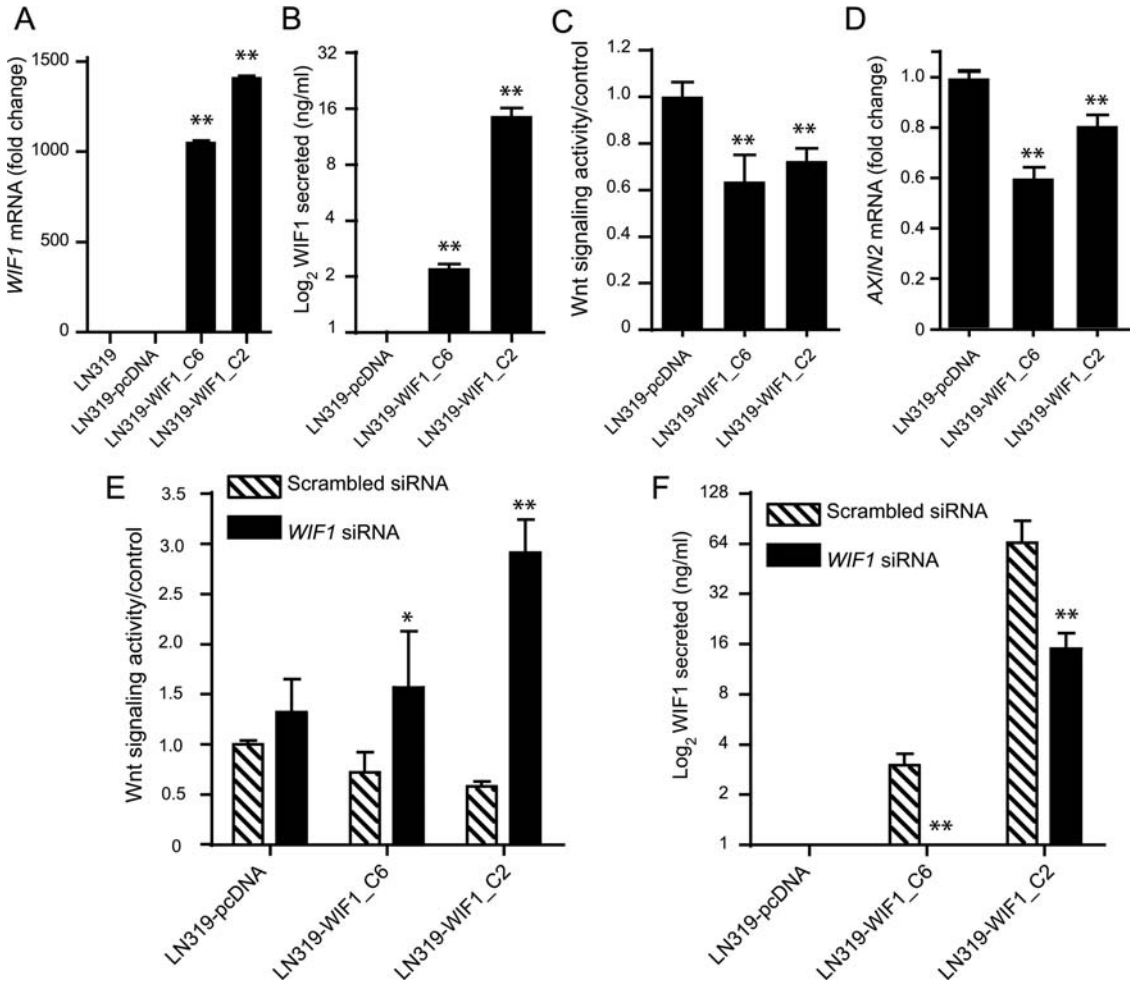


Fig. 4. LN319 cell clones stably transfected with *WIF1* show reduced Wnt pathway signaling. Two stably transfected LN319 clones were analyzed for *WIF1* expression by qRT-PCR (normalized to the control cells transfected with the empty vector, pcDNA3.1) (A) and WIF1 secretion by enzyme-linked immunosorbent assay (ELISA) (B). Wnt pathway signaling was measured both with the TCF luciferase reporter (TOP5/FOP5) and normalized to the control cells (C) and by measuring *AXIN2* mRNA expression (D). The specificity of the WIF1-induced effects in the 2 clones was controlled by transfection of specific siRNAs against *WIF1* or a respective scrambled control. Wnt pathway signaling was measured using the TCF reporter (E) and WIF1 secretion using ELISA (F). Results are marked with 1 asterisk (*) if $P < .05$ and 2 (**) if $P < .01$.

### *WIF1 Expression Decreases Anchorage-Dependent and Anchorage-Independent Growth*

We further investigated the biological effects of WIF1 in the glioblastoma cell lines LN319 and U87. Stably transfected cell clones were characterized for *WIF1* expression and WIF1 secretion and their effect on cell growth (Fig. 4A and B). *WIF1* overexpressing LN319 cells showed reduced Wnt pathway activity ($P < .005$) compared with the respective control cells (Fig. 4C). The downregulation of the canonical pathway was also confirmed by measuring the expression of *AXIN2*, a prototypic Wnt target gene[41] (Fig. 4D). The specificity of the observed effect on the Wnt pathway was determined by silencing of *WIF1* by siRNAs. *WIF1* knockdown indeed rescued transactivation of the TCF reporter in the ectopically expressing *WIF1* LN319 cells, confirming that the detected attenuation of the Wnt pathway was indeed WIF1 dependent (Fig. 4E and F). Glioblastoma cell lines LN229 and U87 were analyzed accordingly. While experiments in LN229 confirmed these results (Supplementary Fig. S3), U87 cells became invariably resistant to ectopic *WIF1* expression over time (passages 20 to 25), although initially sensitive (Fig. 3C). In some cases, clones had lost or attenuated *WIF1* expression/secretion, regardless of continued selection with G418 (Supplementary Fig. S4A). However, most clones gained Wnt pathway activity despite *WIF1* expression and WIF1 secretion. Furthermore, cells were no longer sensitive to knockdown of *WIF1* expression, reflected in no notable increase of pathway activity (Supplementary Fig. S4B and C).

The *WIF1*-expressing cell clones were utilized to investigate the effect of WIF1-mediated downregulation of the Wnt pathway on proliferation. Anchorage-dependent

proliferation measured over 3 days was significantly decreased ($P < .005$) in *WIF1*-overexpressing LN319 clones (Fig. 5A). Even more striking results were obtained investigating the effects on anchorage-independent cell growth. The ability to form colonies in soft agar after 3 weeks of culture was indeed greatly reduced upon *WIF1* overexpression (Fig. 5B and C). During the soft agar experiment, we observed that *WIF1*-overexpressing clones were initially able to proliferate, forming very small clusters of cells, but then stopped dividing after a few days, potentially in response to increasing concentrations of secreted WIF1. In accordance, the colony formation potential was reduced in a *WIF1* dose-dependent manner. The high expressing WIF1 clone LN319-WIF1_C2 displayed 90% fewer colonies, while in the intermediate clone LN319-WIF1_C6, the colony number was reduced by 63%. Similar results were obtained in LN229 (Supplementary Fig. S3A–E). In contrast, the corresponding experiments in *WIF1* stably transduced U87 clones showed initially reduced growth potential that was lost at later passage (passage 4 vs passages 20 to 25) (Supplementary Fig. S4D and E), in line with the observed gain of resistance to WIF1 expression, as detailed above (Supplementary Fig. S4B and C).

### *WIF1 Suppresses Tumorigenicity in a Xenograft Mouse Model*

Ectopic expression of *WIF1* in LN319 cells completely suppressed the inherent tumorigenicity of this glioblastoma cell line. While mice injected with control cells started to develop tumors 25 days after injection, no tumors were detectable in the mice injected with WIF1-expressing cell clones over the observation period of 100 days (Fig. 5D). In contrast, the 2 tested *WIF1*-transduced U87 clones retained tumorigenicity similar to the vector control, in line with development of resistance to WIF1 in vitro. Altogether, these experiments suggest an important role of the Wnt pathway in the development of glioblastoma and a tumor suppressing function for WIF1.

### *WIF1 Overexpression Promotes a Senescence-like Proliferation Arrest*

Observation of *WIF1*-overexpressing cells (LN319 and LN229) until confluence revealed a striking change in morphology. While control cells started to grow on top of each other without apparent contact inhibition, the *WIF1*-expressing cells displayed a phenotype

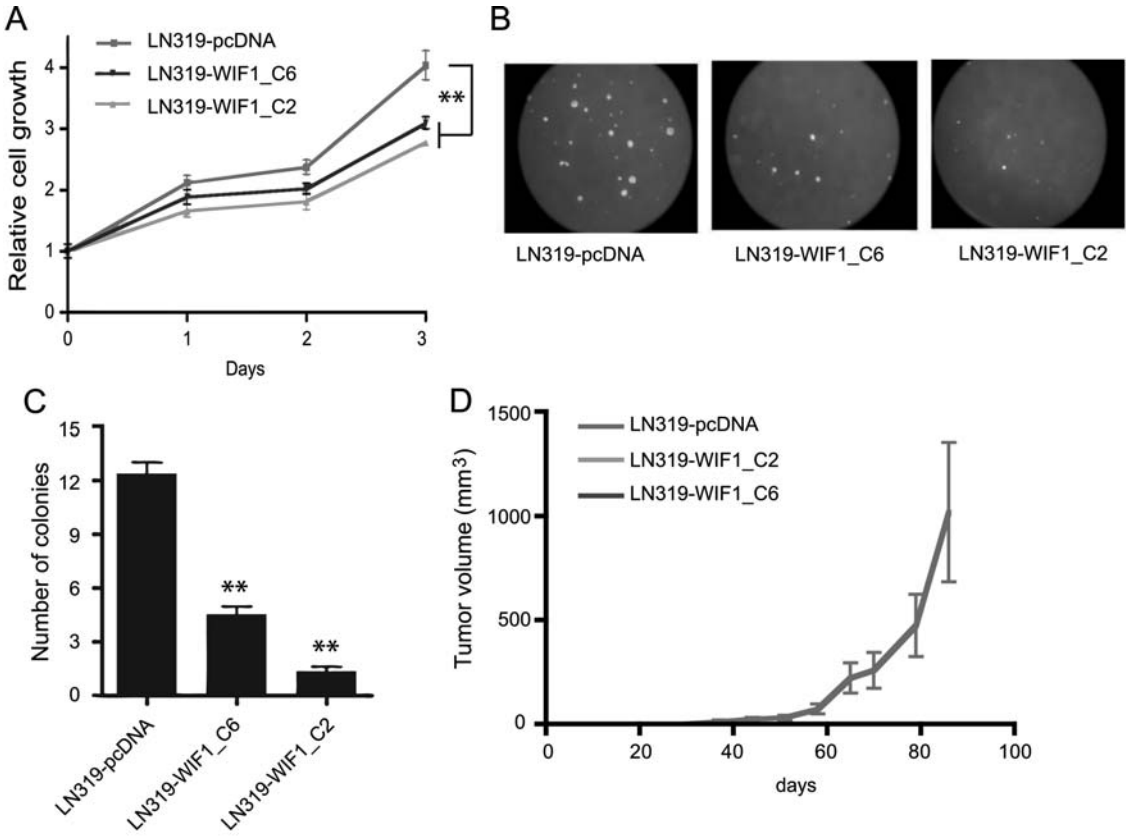


Fig. 5. WIF1 overexpression reduces the growth potential of LN319 cells in vitro and in vivo. Growth of *WIF1*-transduced LN319 clones and the respective empty vector control (pcDNA3.1) was followed over 3 days in culture (A). Anchorage-independent growth was evaluated in soft agar; representative images are shown (B). The average number of colonies counted in 10 randomly chosen fields is reported (C). Tumor growth kinetics of nude mouse xenografts, after subcutaneous injection of WIF1-overexpressing clones and the corresponding empty vector control cells are displayed. The WIF1-overexpressing clones did not form any measurable tumors. The average tumor volume per group (5 mice) is reported (D). Results are marked with 1 asterisk (*) if $P < .05$ and 2 (**) if $P < .01$.

reminiscent of senescent cells with increased cell size. Next we evaluated recognized markers for senescence, including enhanced granularity of the cytoplasm, appearance of multinucleated cells, and presence of senescence-associated β-galactosidase activity.[42,43] Quantification of morphological changes was performed using fluorescence-activated cell sorting analysis. Senescence-like cells were defined as: highly granulated cells = high SS; big cells = high FS. We detected an increased percentage of senescence-like cells in *WIF1*-transfected clones with a positive relationship to WIF1 secretion of the respective clones (Fig. 6A and B, Supplementary Fig. S3F and G). Similar differences were observed upon double staining of the cells with

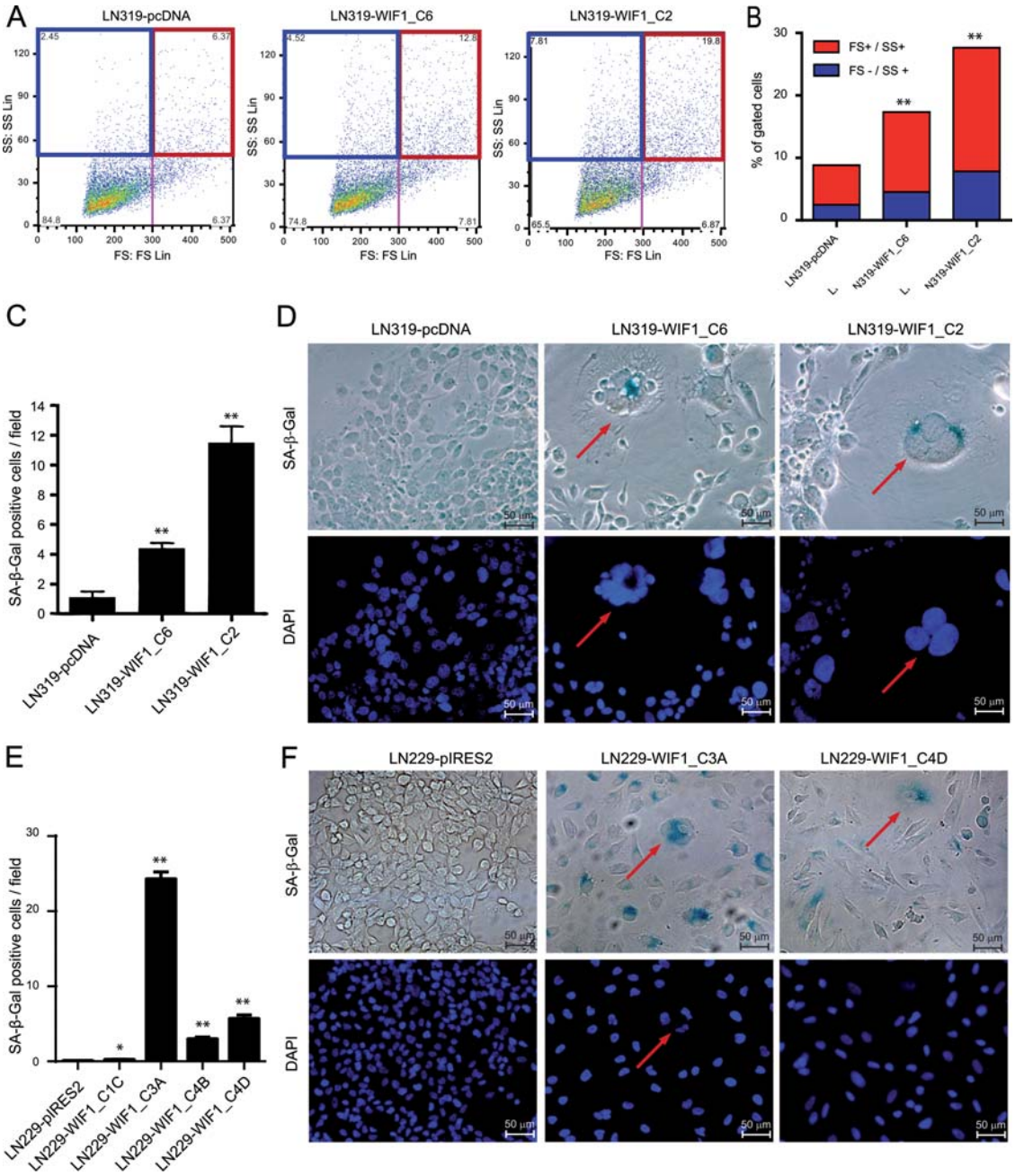


Fig. 6. WIF1 expression and detection of senescence-like cells. Cell morphology of the different LN319 clones was analyzed by fluorescence-activated cell sorting (FACS) (A). Senescence-like cells were defined as highly granulated cells, high side scatter (SS) (blue rectangle), and big cells, high forward scatter (FS) (red rectangle). (B) Quantification of FACS analysis, % of highly granulated cells (SS high, blue), and % of both highly granulated and big cells (FS and SS high, red). Quantification of LN319 (C) and LN229 (E) cells positive for SA-β-galactosidase activity scored in 10 different randomly chosen fields. (D, F) Representative images of clones stained for SA-β-galactosidase and DAPI are shown (200×). Large, SA-β-galactosidase positive (blue) and multinucleated cells are highlighted with red arrows. Results are marked with 1 asterisk (*) if $P < .05$ and 2 (**) if $P < .01$.

SA-β-galactosidase and DAPI, which visualizes nuclear morphology. In the LN319- and LN229-derived WIF1-overexpressing clones, we scored an increased population of both multinucleated and SA-β-galactosidase positive cells (Fig. 6C–F).

## Discussion

Little is known about the role of the Wnt pathway in the malignant behavior of human glioblastoma. Using a combined genomics approach, we provided evidence that the Wnt antagonist *WIF1* is targeted for silencing in glioblastoma, hence represents a good candidate tumor suppressor. In most glioblastomas, *WIF1* silencing is mediated by genomic deletion, promoter hypermethylation, or both. A recent study supports a role for a deregulated Wnt pathway in malignant glioma, showing that additional Wnt pathway inhibitors are epigenetically inactivated, including the family of secreted frizzled-related proteins, dickkopf, and naked.[44] In contrast, mutations in β-catenin (*CTNNB1*) and *APC* are rare in glioblastoma (1/180 and 1/152; https://cma.nci.nih.gov/cma-tcga/geneView/index).[25]

Here we demonstrated that forced *WIF1* expression significantly reduced Wnt signaling in glioblastoma cell lines, while knockdown of *WIF1* induced the pathway. This effect was paralleled by a WIF1 dose-dependent attenuation of cell proliferation in vitro, particularly striking for anchorage-independent growth, and associated with complete abrogation of tumorigenicity. However, the highly malignant glioblastoma cell line U87, although initially sensitive, escaped the effect by either suppressing ectopic expression of *WIF1* or by becoming functionally resistant to WIF1 expression over time, restoring activation of the Wnt pathway. In ephitelial and mesenchymal tumors, a tumor suppressing role for *WIF1* has been proposed. In gastrointestinal cancer cell lines, restoration of WIF1 expression was shown to reduce growth in vitro,[11] and in cell lines from human renal cell carcinoma, prostate cancer, and osteosarcoma WIF1 overexpression has been reported to inhibit tumor growth in vivo.[45–47]

Here, we propose a mechanism by which WIF1 overexpression may exert the growth-inhibiting effect. The WIF1-dependent emergence of enlarged, flattened cells associated with increased detection of SA-β-galactosidase positive, multinucleated cells suggests that WIF1 overexpression induces a senescence-like phenotype in glioblastoma cells. Wnt signaling is involved in diverse processes, from early embryonic patterning[34] to regulation of stem cell self-renewal and differentiation.[48,49] Consequently, Wnt pathway dysregulation can dramatically alter differentiation and cell fate decisions.[50] Recently, Ye et al.[51] reported that downregulation of canonical Wnt signaling was directly associated with the onset of cell senescence in primary human cells. Indeed, in human primary fibroblasts, the process that leads to the formation of senescence-associated heterochromatin foci (SAHF), an early marker of senescence, was initiated upon activation of GSK3β, a key effector of the repressed Wnt signaling pathway.[52] This Wnt-dependent formation of SAHF is independent of the RB1 and TP53 pathways, 2 tumor suppressor pathways frequently inactivated in glioblastoma. Thus, induction of senescence via Wnt pathway inhibition may prove a promising therapeutic strategy.

The CNA patterns reported in this study have a most interesting feature: Most of the glioblastomas with a deletion at the *WIF1* locus have concomitant high-level amplifications of the proto-oncogenes *CDK4* and *MDM2* (Fig. 1C), probably organized extrachromosomally in double minutes. This may suggest that the CNAs of this CHR12q14-15 locus alone, combining co-amplification of *CDK4* and *MDM2* with deletion of the chromosomal region in between, subverts in 1 genetic event 2 important tumor suppressing pathways, the RB- and TP53-pathway, respectively, while simultaneously activating proto-oncogenic Wnt signaling (Fig. 7). Of note, the RB1 and TP53 tumor suppressor pathways are themselves important effectors of senescence. This observation was confirmed in the large TCGA glioblastoma data set (Supplementary Fig. S1) and underlines the need for concerted targeting of signaling pathways that cooperate in glioblastoma, including the Wnt pathway. Specific inhibitors for CDK4 and MDM2 are in clinical development.[53] Small molecule inhibitors targeting the Wnt pathway by novel mechanisms have been proposed recently. They comprise inhibitors of Wnt production by targeting Porcn, and inhibitors of Wnt response that stabilize Axin, promoting the association of β-catenin with the destruction complex,[54,55] or β-catenin interaction disruptors

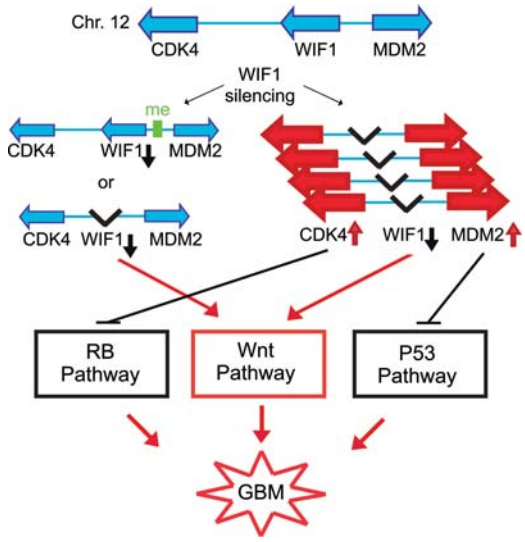


Fig. 7. Model for mechanisms implicated in deregulation of both tumor suppressing and proto-oncogenic pathways on chromosome 12. The model suggests that deletion at the *WIF1* locus, if concomitant with amplification of the proto-oncongenes *CDK4* and *MDM2,* can subvert the important tumor suppressing pathways regulated by RB1 and TP53 while simultaneously activating proto-oncogenic Wnt signaling.

preventing β-catenin from associating with TCF or cAMP response element binding. The observation of frequent inactivation of genes coding for secreted Wnt antagonists in glioma may favor the use of inhibitors of Wnt production or the development of molecules sequestering Wnt family members. Such intervention may have the additional advantage of interfering with tumor angiogenesis, since the ligands Wnt7a/7b have been shown to be involved in brain angiogenesis and induction of the blood-brain barrier, both relevant factors for glioma vascularization and therapy.[56]

The present study provides the rationale for investigating inhibitors of Wnt signaling in glioblastoma as a new avenue for individualized therapy. The addition of a Wnt pathway inhibitor to the current standard of care of combined radiochemotherapy with the alkylating agent temozolomide may improve outcomes particularly in patients whose tumors carry a methylated *MGMT* promoter,[15] due to the significant association with *WIF1* methylation. However, the importance of the Wnt pathway that is interlinked with other mitogenic pathways may rapidly select for resistance in a corresponding single-agent therapy, as suggested by the experiments with the highly malignant glioblastoma cell line U87.

## Supplementary Material

Supplementary material is available online at *Neuro-Oncology* (http://neuro-oncology.oxfordjournals.org/).

## Acknowledgments

We are indebted to the patients for consenting to donate their tumor tissue for translational research. We thank Dr. Vincent Castella for excellent technical support.

*Conflict of interest statement*. None declared.

## Funding

Nélia and Amadeo Barletta Foundation (W.L.L., M.E.H., R.S.), The Brain Tumor Funders Cooperative (M.E.H), and the National Center of Competence in Research Molecular Oncology (M.E.H., E.M., M.D., A.M.), Swiss National Science Foundation (31003A_122557, M.E.H., M.D., I.V.), and the Leir Charitable Foundation (T.S., E.D.).

## References

1. Stupp R, Hegi ME, Mason WP, et al. Effects of radiotherapy with concomitant and adjuvant temozolomide versus radiotherapy alone on survival in glioblastoma in a randomised phase III study: 5-year analysis of the EORTC-NCIC trial. *Lancet Oncol*. 2009;10(5):459–466.
2. Ein-Dor L, Zuk O, Domany E. Thousands of samples are needed to generate a robust gene list for predicting outcome in cancer. *Proc Natl Acad Sci USA*. 2006;103(15):5923–5928.
3. McLendon R, Friedman A, Bigner D, et al. Comprehensive genomic characterization defines human glioblastoma genes and core pathways. *Nature*. 2008;455(7216):1061–1068.
4. Parsons DW, Jones S, Zhang X, et al. An integrated genomic analysis of human glioblastoma multiforme. *Science*. 2008;321(5897):1807–1812.
5. Murat A, Migliavacca E, Gorlia T, et al. Stem cell-related "self-renewal" signature and high epidermal growth factor receptor expression associated with resistance to concomitant chemoradiotherapy in glioblastoma. *J Clin Oncol*. 2008;26(18):3015–3024.
6. Stupp R, Mason WP, van den Bent MJ, et al. Radiotherapy plus concomitant and adjuvant temozolomide for glioblastoma. *N Engl J Med*. 2005;352(10):987–996.
7. Stupp R, Dietrich P, Ostermann Kraljevic S, et al. Promising survival for patients with newly diagnosed glioblastoma multiforme treated with concomitant radiation plus temozolomide followed by adjuvant temozolomide. *J Clin Oncol*. 2002;20(5):1375–1382.
8. Reifenberger G, Ichimura K, Reifenberger J, Elkahloun AG, Meltzer PS, Collins VP. Refined mapping of 12q13-q15 amplicons in human malignant gliomas suggests CDK4/SAS and MDM2 as independent amplification targets. *Cancer Res*. 1996;56(22):5141–5145.
9. Hsieh JC, Kodjabachian L, Rebbert ML, et al. A new secreted protein that binds to Wnt proteins and inhibits their activities. *Nature*. 1999;398(6726):431–436.
10. Kawano Y, Kypta R. Secreted antagonists of the Wnt signalling pathway. *J Cell Sci*. 2003;116(Pt 13):2627–2634.
11. Taniguchi H, Yamamoto H, Hirata T, et al. Frequent epigenetic inactivation of Wnt inhibitory factor-1 in human gastrointestinal cancers. *Oncogene*. 2005;24(53):7946–7952.
12. Urakami S, Shiina H, Enokida H, et al. Epigenetic inactivation of Wnt inhibitory factor-1 plays an important role in bladder cancer through aberrant canonical Wnt/beta-catenin signaling pathway. *Clin Cancer Res*. 2006;12(2):383–391.
13. Yang Z, Wang Y, Fang J, Chen F, Liu J, Wu J. Expression and aberrant promoter methylation of Wnt inhibitory factor-1 in human astrocytomas. *J Exp Clin Cancer Res*. 2010;29:26.
14. Schutz F, Delorenzi M. MAMOT: hidden Markov modeling tool. *Bioinformatics*. 2008;24(11):1399–1400.
15. Hegi ME, Diserens AC, Gorlia T, et al. MGMT gene silencing and benefit from temozolomide in glioblastoma. *New Engl J Med*. 2005;352(10):997–1003.
16. Murat A, Migliavacca E, Hussain SF, et al. Modulation of angiogenic and inflammatory response in glioblastoma by hypoxia. *PLoS ONE*. 2009;4(6):e5947.
17. Andreeff M, Ruvolo V, Gadgil S, et al. HOX expression patterns identify a common signature for favorable AML. *Leukemia*. 2008;22(11):2041–2047.
18. Lal M, Song X, Pluznick JL, et al. Polycystin-1 C-terminal tail associates with beta-catenin and inhibits canonical Wnt signaling. *Hum Mol Genet*. 2008;17(20):3105–3117.
19. Ishii N, Maier D, Merlo A, et al. Frequent co-alterations of TP53, p16/CDKN2A, p14ARF, PTEN tumor suppressor genes in human glioma cell lines. *Brain Pathol*. 1999;9(3):469–479.
20. Lorenzi PL, Reinhold WC, Varma S, et al. DNA fingerprinting of the NCI-60 cell line panel. *Mol Cancer Ther*. 2009;8(4):713–724.

21. Foltz G, Ryu GY, Yoon JG, et al. Genome-wide analysis of epigenetic silencing identifies BEX1 and BEX2 as candidate tumor suppressor genes in malignant glioma. *Cancer Res*. 2006;66(13):6665–6674.
22. Hatzis P, van der Flier LG, van Driel MA, et al. Genome-wide pattern of TCF7L2/TCF4 chromatin occupancy in colorectal cancer cells. *Mol Cell Biol*. 2008;28(8):2732–2744.
23. Chan SL, Cui Y, van Hasselt A, et al. The tumor suppressor Wnt inhibitory factor 1 is frequently methylated in nasopharyngeal and esophageal carcinomas. *Lab Invest*. 2007;87(7):644–650.
24. You L, He B, Xu Z, et al. Inhibition of Wnt-2-mediated signaling induces programmed cell death in non-small-cell lung cancer cells. *Oncogene*. 2004;23(36):6170–6174.
25. The Cancer Genome Atlas Consortium. Comprehensive genomic characterization defines human glioblastoma genes and core pathways. *Nature*. 2008;455(7216):1061–1068.
26. Freije WA, Castro-Vargas FE, Fang Z, et al. Gene expression profiling of gliomas strongly predicts survival. *Cancer Res*. 2004;64(18):6503–6510.
27. Rich JN, Hans C, Jones B, et al. Gene expression profiling and genetic markers in glioblastoma survival. *Cancer Res*. 2005;65(10):4051–4058.
28. Phillips HS, Kharbanda S, Chen R, et al. Molecular subclasses of high-grade glioma predict prognosis, delineate a pattern of disease progression, and resemble stages in neurogenesis. *Cancer Cell*. 2006;9(3):157–173.
29. Sun L, Hui AM, Su Q, et al. Neuronal and glioma-derived stem cell factor induces angiogenesis within the brain. *Cancer Cell*. 2006;9(4):287–300.
30. Horvath S, Zhang B, Carlson M, et al. Analysis of oncogenic signaling networks in glioblastoma identifies ASPM as a molecular target. *Proc Natl Acad Sci USA*. 2006;103(46):17402–17407.
31. Laffaire J, Everhard S, Idbaih A, et al. Methylation profiling identifies 2 groups of gliomas according to their tumorigenesis. *Neuro Oncol*. 2010;2010:8.
32. Yang Z, Wang Y, Fang J, et al. Downregulation of WIF-1 by hypermethylation in astrocytomas. *Acta Biochim Biophys Sin (Shanghai)*. 2010;42(6):418–425.
33. Nusse R, Varmus HE. Many tumors induced by the mouse mammary tumor virus contain a provirus integrated in the same region of the host genome. *Cell*. 1982;31(1):99–109.
34. Moon RT, Brown JD, Torres M. WNTs modulate cell fate and behavior during vertebrate development. *Trends Genet*. 1997;13(4):157–162.
35. Forbes SA, Tang G, Bindal N, et al. COSMIC (the Catalogue of Somatic Mutations in Cancer): a resource to investigate acquired mutations in human cancer. *Nucleic Acids Res*. 2010;38(Database issue):D652–D657.
36. Hegi ME, Liu L, Herman JG, et al. Correlation of O6-methylguanine methyltransferase (MGMT) promoter methylation with clinical outcomes in glioblastoma and clinical strategies to modulate MGMT activity. *J Clin Oncol*. 2008;26(25):4189–4199.
37. Hegi ME, Diserens AC, Godard S, et al. Clinical trial substantiates the predictive value of O-6-methylguanine-DNA methyltransferase promoter methylation in glioblastoma patients treated with temozolomide. *Clin Cancer Res*. 2004;10(6):1871–1874.
38. Vlassenbroeck I, Califice S, Diserens AC, et al. Validation of real-time methylation-specific PCR to determine O6-methylguanine-DNA methyltransferase gene promoter methylation in glioma. *J Mol Diagn*. 2008;10(4):332–337.
39. Beier CP, Schmid C, Gorlia T, et al. Pegylated liposomal doxorubicine and prolonged temozolomide in addition to radiotherapy in newly diagnosed glioblastoma - a phase II study. *BMC Cancer*. 2009;9:308.
40. Hegi ME, zur Hausen A, Ruedi D, Malin G, Kleihues P. Hemizygous or homozygous deletion of the chromosomal region containing the p16INK4a gene is associated with amplification of the EGF receptor gene in glioblastomas. *Int J Cancer*. 1997;73(1):57–63.
41. Jho E-h, Zhang T, Domon C, Joo C-K, Freund J-N, Costantini F. Wnt/{beta}-Catenin/Tcf Signaling Induces the Transcription of Axin2, a Negative Regulator of the Signaling Pathway. *Mol Cell Biol*. 2002;22(4):1172–1183.
42. Matsumura T. Multinucleation and polyploidization of aging human cells in culture. *Adv Exp Med Biol*. 1980;129:31–38.
43. Chang BD, Broude EV, Dokmanovic M, et al. A senescence-like phenotype distinguishes tumor cells that undergo terminal proliferation arrest after exposure to anticancer agents. *Cancer Res*. 1999;59(15):3761–3767.
44. Gotze S, Wolter M, Reifenberger G, Muller O, Sievers S. Frequent promoter hypermethylation of Wnt pathway inhibitor genes in malignant astrocytic gliomas. *Int J Cancer*. 2010;126(11):2584–2593.
45. Kawakami K, Hirata H, Yamamura S, et al. Functional significance of Wnt inhibitory factor-1 gene in kidney cancer. *Cancer Res*. 2009;69(22):8603–8610.
46. Yee DS, Tang Y, Li X, et al. The Wnt inhibitory factor 1 restoration in prostate cancer cells was associated with reduced tumor growth, decreased capacity of cell migration and invasion and a reversal of epithelial to mesenchymal transition. *Mol Cancer*. 2010;9(1):162.
47. Rubin EM, Guo Y, Tu K, Xie J, Zi X, Hoang BH. Wnt inhibitory factor 1 decreases tumorigenesis and metastasis in osteosarcoma. *Mol Cancer Ther*. 2010;9(3):731–741.
48. van de Wetering M, Sancho E, Verweij C, et al. The beta-catenin/TCF-4 complex imposes a crypt progenitor phenotype on colorectal cancer cells. *Cell*. 2002;111(2):241–250.
49. Reya T, Clevers H. Wnt signalling in stem cells and cancer. *Nature*. 2005;434(7035):843–850.
50. Boerboom D, White LD, Dalle S, Courty J, Richards JS. Dominant-stable beta-catenin expression causes cell fate alterations and Wnt signaling antagonist expression in a murine granulosa cell tumor model. *Cancer Res*. 2006;66(4):1964–1973.
51. Ye X, Zerlanko B, Kennedy A, Banumathy G, Zhang R, Adams PD. Downregulation of Wnt signaling is a trigger for formation of facultative heterochromatin and onset of cell senescence in primary human cells. *Mol Cell*. 2007;27(2):183–196.
52. Ali A, Hoeflich KP, Woodgett JR. Glycogen synthase kinase-3: properties, functions, and regulation. *Chem Rev*. 2001;101(8):2527–2540.
53. Benouaich-Amiel A, Mazza E, Massard C, et al. Phase I study of the oral CDK-TRKA inhibitor PHA-848125 in recurrent malignant glioma (MG). *J Clin Oncol (Meeting Abstracts)*. 2010;28(15 suppl):2087.
54. Chen B, Dodge ME, Tang W, et al. Small molecule-mediated disruption of Wnt-dependent signaling in tissue regeneration and cancer. *Nat Chem Biol*. 2009;5(2):100–107.
55. Lu J, Ma Z, Hsieh JC, et al. Structure-activity relationship studies of small-molecule inhibitors of Wnt response. *Bioorg Med Chem Lett*. 2009;19(14):3825–3827.
56. Liebner S, Plate KH. Differentiation of the brain vasculature: the answer came blowing by the Wnt. *J Angiogenes Res*. 2010;2(1):1.
57. Tsafrir D, Tsafrir I, Ein-Dor L, Zuk O, Notterman DA, Domany E. Sorting points into neighborhoods (SPIN): data analysis and visualization by ordering distance matrices. *Bioinformatics*. 2005;21(10):2301–2308. Epub 2005 Feb 2318.